

CONDENSATION OF MIXTURES GIVING TWO
IMMISCIBLE LIQUID PHASES

By

ANIL VASANT GOKHALE

Bachelor of Chemical Engineering

University of Bombay

Bombay, India

1980

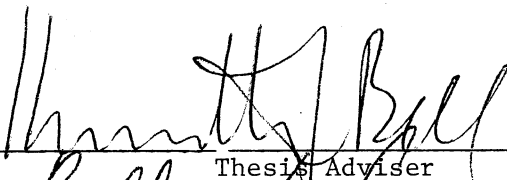
Submitted to the Faculty of the Graduate College
of the Oklahoma State University
in partial fulfillment of the requirements
for the Degree of
MASTER OF SCIENCE
December, 1982

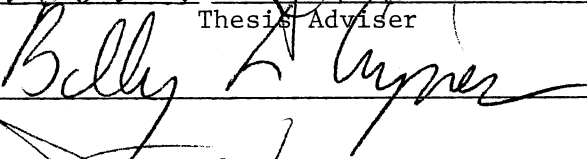
Thesis
1982
G616C
cop. 2

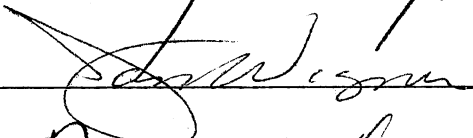


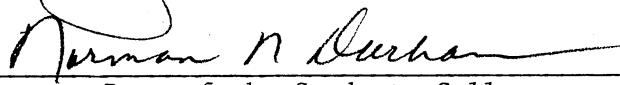
CONDENSATION OF MIXTURES GIVING TWO
IMMISCIBLE LIQUID PHASES

Thesis Approved:



Thesis Adviser






Dean of the Graduate College

PREFACE

Condensation of multicomponent vapor may result in the formation of two liquid phases immiscible with one another. Predicting the heat transfer rates across the condensate layer is complicated because of its complex and unpredictable structure. This work initiates a major study on this problem. The equipment design and set up is done and various experimental and photographic techniques are established.

I wish to express my sincere thanks to Dr. Kenneth J. Bell for his advice and guidance during this work and on various other matters. Important suggestions by Dr. Billy L. Crynes and Dr. Jan Wagner are sincerely appreciated. It is a pleasure to thank Dr. Mayis Seapan for the financial assistance. I also express my sincere gratitude to Suresh Balakrishnan and Summer Dale for their help and everlasting encouragement. Finally, I wish to thank Teresa Tackett for a typing job well done in a short time.

TABLE OF CONTENTS

Chapter	Page
I. INTRODUCTION	1
Condensation	2
Nature of the Problem	3
II. LITERATURE REVIEW.	7
Investigation Using Horizontal Tubes	7
Investigation Using Vertical Tubes.	13
Investigation Using Other Geometries	17
Summary	20
III. APPARATUS.	22
Introduction.	22
Vapor Side System	24
Vapor Generation	24
Condensation Cell.	25
Auxiliary Condenser.	28
Cooling System.	30
Pumps.	30
Rotameters	32
Piping System.	32
Temperature Measurement	33
Photography	34
IV. EXPERIMENTAL PROCEDURE	36
V. DATA ANALYSIS.	39
Data on Steam	39
Data on Toluene-Water System.	42
Visual Observations	47
VI. CONCLUSIONS AND RECOMMENDATIONS.	56
BIBLIOGRAPHY.	57
APPENDIXES.	60

Chapter	Page
APPENDIX A - ANALYSIS OF FILMWISE CONDENSATION.	61
APPENDIX B - SUMMARY OF VARIOUS INVESTIGATIONS.	64
APPENDIX C - ROTAMETER CALIBRATION.	69
APPENDIX D - CALCULATIONS FOR STEAM CONDENSATION.	71
APPENDIX E - CALCULATIONS FOR TOLUENE-WATER CONDENSATION. . .	74

LIST OF TABLES

Table	Page
I. Results from Steam Runs	40
II. Results from Toluene-Water Runs	44
III. Data on Toluene-Water Runs	79

LIST OF FIGURES

Figure	Page
1. Eutectic Diagram	5
2. Schematic Flow Diagram	23
3. Assembled Test Cell.	26
4. Sketch of the Plate.	29
5. Auxiliary Condenser.	31
6. Effect of Noncondensibles on Condensing Coefficient.	41
7. Heat Transfer Coefficient as a Function of the Film Temperature Difference	45
8. Comparison Between the Experimental and Predicted Values of the Heat Transfer Coefficients.	46
9. Dropwise Condensation of Steam	48
10. Filmwise Condensation of Steam	48
11. Dropwise Condensation Sequence Frame 1	49
12. Dropwise Condensation Sequence Frame 2	49
13. Dropwise Condensation Sequence Frame 3	50
14. Dropwise Condensation Sequence Frame 4	50
15. Dropwise Condensation Sequence Frame 5	51
16. Toluene-Water Condensation-1	51
17. Toluene-Water Condensation-2	52
18. Toluene-Water Condensation-3	52
19. Toluene-Water Condensation-4	53

Figure	Page
20. Toluene-Water Condensation-5.	53
21. Toluene-Water Condensation-6.	54
22. Toluene-Water Condensation-7.	54
23. Filmwise Condensation	62

CHAPTER I

INTRODUCTION

Condensation

Condensation of immiscible mixtures is encountered in a variety of process and related industries. The mixtures vary from crude oil-water to turpentine gum-water to styrene-butadiene-water. In the majority of the cases, one of the immiscible phases is aqueous. However, the mechanism of condensation from mixed vapors into two (or more) immiscible liquid phases is not fully understood.

In 1916, Nusselt published the first sound theoretical development to calculate the heat transfer coefficients for the condensation of a single component. Nusselt made a series of assumptions, such as laminar flow of condensate film, no vapor shear, etc. and arrived at the following two equations to calculate the condensing heat transfer coefficient.

For a single horizontal tube with condensation on the outside surface:

$$h = 0.725 \left[\frac{k_\ell^3 \rho_\ell^2 g \lambda}{\Delta t_f \mu_\ell D} \right]^{0.25} \quad (1.1)$$

and for a vertical tube,

$$h = 0.943 \left[\frac{k_\ell^3 \rho_\ell^2 g \lambda}{\Delta t_f \mu_\ell L} \right]^{0.25} \quad (1.2)$$

where:

k_ℓ = thermal conductivity of the liquid film,

ρ_ℓ = density of the liquid film,

g = gravitational acceleration,

λ = latent heat of condensation,

Δt_f = temperature drop across the condensate film,

μ_ℓ = viscosity of the condensate film,

D = diameter of the tube and

L = length of the tube.

Numerous results have been published after 1916 to show how the heat transfer coefficient is affected when one or more of Nusselt's assumptions break down. To cite two examples, among others, the effect of turbulence was studied by Colburn (11), and the vapor shear effect by Boyko and Kruzhilin (10).

In the case of condensation of immiscible mixtures, one of the most frequently violated of Nusselt's assumptions is that of a continuous film of condensate. A large number of condensation patterns are reported. The two basic patterns, namely, dropwise and filmwise, observed in the case of a single component, can be imagined to form various combinations during the condensation of two immiscible liquid phases. The mechanism of dropwise condensation for the case of a single component itself is not fully understood. Hence, the addition of another liquid phase gives rise to still more uncertainty.

The mechanism of filmwise condensation is quite well understood. An illustration is given in Appendix A. The original treatment of Nusselt is analyzed by Kern (18) and Jakob (16) extensively.

Dropwise condensation has been a subject of interest for a long time because of the high heat transfer coefficients observed. The heat transfer coefficients observed are as high as ten times those calculated by Nusselt's equation. Several theories have been proposed to explain this phenomenon. Bernhardt (6) has covered the subject quite comprehensively. He also has shown photographic evidence to support the nucleation theory. A series of photographs showing nucleation in progress is presented in Chapter V. These are for condensation of pure steam. These photographs also support Bernhardt's analysis.

Nature of the Problem

When a mixture of immiscible liquids is heated together in the same vessel, each of the liquids will exert its own vapor pressure. When the sum of the vapor pressures reaches the total pressure, boiling will start, resulting in a eutectic vapor mixture. Gibb's phase rule can be stated as:

$$F + P = C + 2 \quad (1.3)$$

where:

F = degrees of freedom,

P = number of phases, and

C = number of components.

In the process of boiling, we have two components in two liquid phases, plus a vapor phase. This leads to only one degree of freedom, namely, pressure, or alternatively, temperature. Hence, boiling of the two liquids together will, in theory, always result in a vapor phase of eutectic composition. If a vapor mixture with a composition other

than eutectic is needed, the two liquid phases must be boiled separately, and the vapors mixed.

During condensation, if the vapor composition is eutectic, the condensate will also have the same composition. This is represented by point E in Figure 1. However, if the vapor is richer in one component, that component will condense first selectively, till the vapor phase attains the eutectic composition. This is indicated by transformation from point A or B to point E in Figure 1. Hence, in this case, the bulk of the condensate collected will not be a eutectic mixture.

Various condensing patterns have been reported. A detailed description is given in Chapter II. Several empirical equations have been proposed. However, there is not a single reported work which predicts the heat transfer coefficients from first principles. Designs have been done by using rules of thumb and results from single component condensation.

It is expected that when two liquid phases and one metal surface are in contact, the interfacial tensions will play a dominant role in deciding the condensation patterns, and hence the heat transfer coefficients (henceforth referred to as coefficients). None of the reported equations include any term accounting for interfacial tensions. The effect of vapor shear has not been studied either, though it is more important at this stage to work with a minimum number of variables to study the coefficients and the condensing patterns.

This is the first step of a major study intended on this problem. In this work, the design of equipment is done along with acquiring and setting up the same. Experiments are done first with one pure

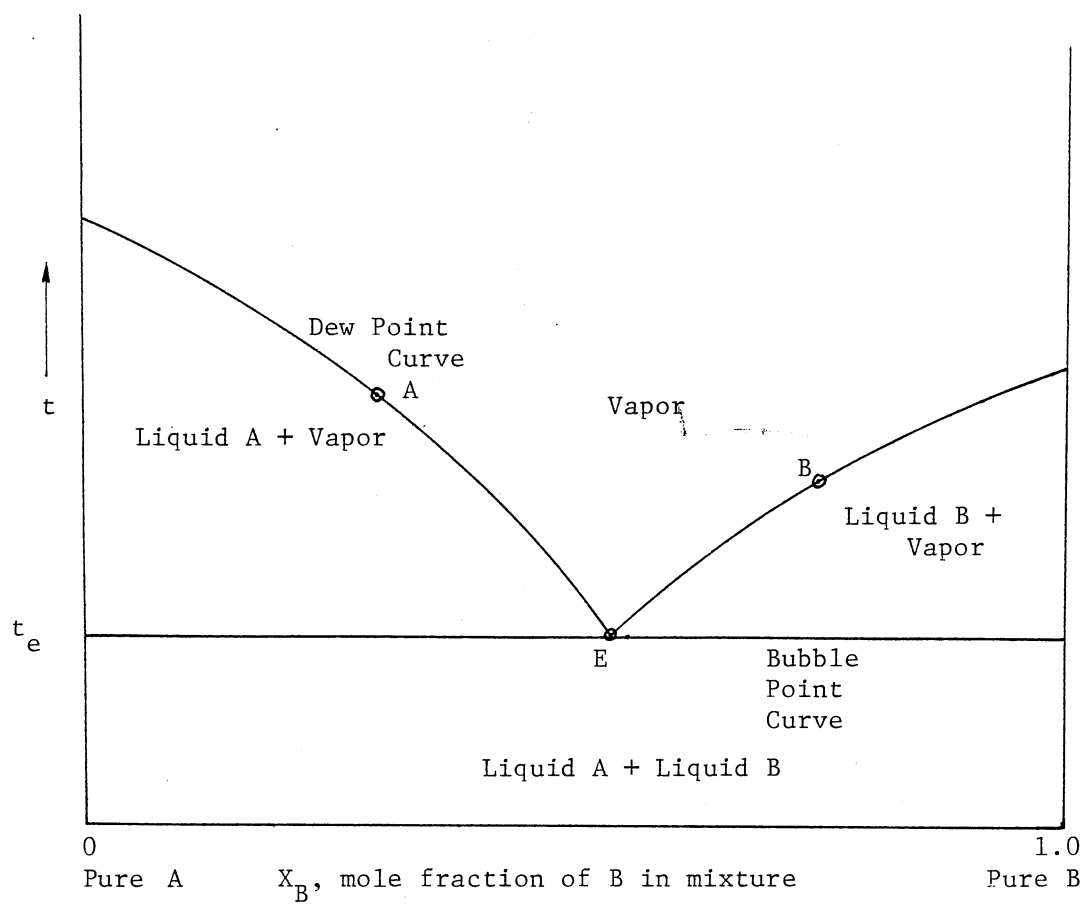


Figure 1: Eutectic Diagram

component (water) and then with a mixture of vapors (toluene and water). Experimental techniques are established and methods are worked out to deal with the practical difficulties involved in the experimental procedure. Special techniques are developed for still as well as motion photography. The data obtained agree well with the published data.

Future work will be aimed at determining whether a "flow regime map" can be constructed whereby the liquid structure and its heat transfer characteristics can be related to the sequence of formation of the two phases, the amounts and properties of the individual phases, the geometry of the system and the magnitude and direction of vapor shear on the interface.

CHAPTER II

LITERATURE REVIEW

Investigation Using Horizontal Tubes

In 1933, Kirkbride (19) published the first reported work on the subject of binary condensation. His experiments dealt with two mixtures, namely, benzene-steam and "cleaners naphtha"-steam. It was recognized that 'drop forming condensation' could have occurred and complicated the problem. An average heat transfer coefficient was calculated using the heat loads of the two components as the weighting factors. The equation can be written as:

$$h_m = \frac{h_s Q_s + h_o Q_o}{Q_s + Q_o} \quad (2.1)$$

where:

h_m = mean heat transfer coefficient,

h_o = coefficient for organic phase (calculated by Nusselt equation on the assumption that only the organic was condensing on the entire surface),

h_s = coefficient for steam (calculated by Nusselt equation on the assumption that only the steam was condensing on the entire surface),

Q_s = heat load for steam, and

Q_o = heat load for organic phase.

While calculating the pure component condensing coefficients, equation 1.1 or 1.2 was used. The properties of the pure components were used along with the film temperature difference observed during binary condensation.

No attempt was made to ensure that the vapors were of eutectic composition. In fact, it was reported that the uncondensed vapor leaving the test section was superheated. A horizontal internally cooled tube was used as the condensing test surface. Also, the temperature variation around the periphery of the tube was ignored.

Baker and Mueller (3) studied benzene, toluene, mixed heptanes and trichloroethylene as the organic phases along with steam. Though they attempted to get eutectic mixtures, they reported a substantial amount of data on non-eutectic compositions. After a series of mathematical manipulations, they obtained the following equation:

$$h \left[\frac{\mu^2}{k_{av}^3 \rho_{av}^2 g} \right]^{1/3} = 1.28 \left[\frac{C_{p_{av}} \mu \rho_{av}^{0.7}}{k_{av} \lambda_{av}} \right]^{2.38} \left(\frac{Q_s}{Q} \right)^{-3.28} \quad (2.2)$$

where:

ρ_{av} = average liquid density based on weight fraction in the condensate, lb/cubic ft.,

$C_{p_{av}}$ = average specific heat of condensate based on weight fraction in the condensate, Btu/lb-deg F,

λ_{av} = average latent heat of condensation based on weight fraction in the condensate, Btu/lb,

k_{av} = average thermal conductivity of condensate based on volume fraction in the condensate, Btu/hr-ft-deg F,

μ = viscosity of the film forming component (organic) lb/ft-hr,

Q_s = steam heat load, and

Q = total heat load

The equation is not dimensionally consistent and should be used in only the given system of units. It was concluded that at that time, 'a strictly theoretical attack' on the problem was not possible. Thermal and physical properties of the liquids, as well as the surface properties, would be important.

Baker and Tsao (4) used the electrical resistance method for measuring the surface temperature, and used an average value over the entire length of the tube as well as around the periphery. They calculated the temperature drop across the tube wall from the heat load and assumed it to be uniform around the circumference. The equations suggested are highly empirical and give absurd values if the parameters are used beyond their suggested range.

Baker, Mueller and Tsao have indicated no change in the heat transfer coefficients with change in film temperature difference. The temperature difference varied from 7 to 70 deg F. However, Patton and Feagan (24) clearly showed that this was not true and presented a graph with $h_f \propto (\Delta t_f)^{-0.5}$. This was supported by Sykes and Marchello (28).

Stepanek and Standart (27) did some theoretical development but they could not arrive at a conclusive equation because of mathematical difficulties. They have presented a semi-theoretical equation. Bernhardt et al. (7) pointed out that the Stepanek-Standart equation breaks down for pure substances and shows a zero heat transfer coefficient for an intermediate composition. Also, it does not fit very well with the data of others. They point out that the dependence of h on the

film temperature difference varies with the substance in question. They studied benzene, toluene, dichlorethane and chlorobenzene along with water.

The equation proposed by Sykes and Marchello (28) gives the same heat transfer coefficient as for a pure organic, if the density of the organic phase is same as that of water. However, there are no data available to support this. The dependence of h on film temperature difference was considered to be varying in accordance with the density of the organic phase. This was found not to be always true and later was associated with the condensation patterns by Polley and Calus (25). The second correlation of Sykes and Marchello is based on the two-film model and assumes that the organic film is adjacent to the wall and the water film is on top of the organic. This was expected to give minimum heat transfer coefficients, but failed to do so. Their third equation, based on the nucleation model, was the most successful over a wide range of systems. It assumed an organic film on the surface and the water drops nucleating on it. The equations are given in Appendix B.

Kawasaki et al. (17) studied simultaneous mass and heat transfer effects, using the Maxwell equations for mass transfer. They suggest the following correlations on the lines of the Nusselt equation:

$$Nu = 0.0295 (GaKuPr)^{1/4} Re_v^{1/2} \quad (2.3)$$

where:

$$Ga = \text{Gallileo number} = \frac{D^3 \rho^2 g}{\mu^2} \quad \text{and}$$

$$Ku = \text{Kutateladze number} = \frac{\lambda}{C_p \Delta t_f}$$

It is apparent from the sketch of their apparatus that the vapor flowed across the tube with a possibility of vapor shear. Nusselt's development assumes negligible vapor shear. Also, they have shown one thermocouple each for measuring the surface temperature and the vapor temperature. The tube could not be rotated on its axis and hence they have neglected the effect of temperature variation around the tube. They use average properties of the condensate. Thermal conductivity, density, and viscosity are based on volume fractions and the specific heat is based on the weight fraction.

Salov and Danilov (26) have studied the temperature variation around the periphery of a horizontal tube and along the length of a vertical tube. Based on these, they have presented analytical equations for local and mean values of heat transfer coefficients. The mixtures studied were benzene, toluene, trichlorethane, heptane, turpentine and gasoline along with water.

Bernea and Mizrahi (5) have argued that correlating the heat transfer coefficient to the film temperature difference is not correct. They have come up with a proportionality as:

$$h \propto \left(\frac{Q}{A} \right)^{1.26} \quad (2.4)$$

Replacing $\left(\frac{Q}{A} \right)$ by $(h\Delta t_f)$ leads to $h \propto (\Delta t_f)^{-4.84}$.

Their study involves back-calculating the condensing heat transfer coefficient from the overall heat transfer coefficient. They have calibrated the coolant side coefficient to the Reynolds number of the coolant

flow at a particular value of Q/A . This was then used for all further calculations at various values of Q/A . There may be inherent changes in the coolant side coefficient as more and more experiments are done, due to scaling, dirt film formation, etc. Further, when the coolant side resistance has a dominant effect on the overall heat transfer coefficient, small errors in its value will lead to large errors in the calculation of condensing coefficients. There are too many variables involved and the approach itself is questionable.

Yusufova and Neidukht (30) have studied complete and partial condensation of gasoline and water vapor inside horizontal tubes, with vapor velocities up to 15 m/s (50 f/s). They report that the condensing heat transfer coefficient is independent of the tube material and increases with a increase in the specific heat flux Q/A . The degree of finish of the tube surface has a considerable effect on the heat transfer coefficient. They report a proportionality as:

$$h \propto \left(\frac{Q}{A}\right)^{1.1} \quad (2.5)$$

In this case substituting (Q/A) by $(h \Delta t_f)$ will result in:

$$h \propto (\Delta t_f)^{-1.1}$$

They also present a curve with decreasing h with a increasing film temperature difference. It is well accepted that the heat transfer coefficient during the condensation of immiscible mixtures is dependent on the condensing patterns, or at least, changes with changing patterns. In the work of Yusufova and Neidukht, the vapor velocities are likely to affect the condensing patterns. Hence, their

data are not very useful for studying the effect of one parameter at a time.

Investigation Using Vertical Tubes

Patterson et al. (23) worked with a heptane-water mixture at low water contents by injecting live steam into heptane. There was no attempt made to control the composition of the mixed vapors. The water was observed to condense in a dropwise manner, and the heptane formed rivulets or a film. No correlation was given to calculate the heat transfer coefficient.

Hazelton and Baker (15) started with a theoretical development based on Nusselt's equation. Though with this they were not able to correlate the data successfully, empirical correlations were arrived at based on the theoretical equations. Modifying the equipment of Baker and Tsao for a vertical tube, experiments were done for water with benzene, toluene and chlorobenzene. Also a correlation was presented for the data available on horizontal tubes. Hazelton and Baker have postulated six different types of flow patterns as quoted here.

Flow type 1 (Film-drop) - The organic liquid completely wets the condensing surface, forming a continuous film which displaces the water from any point at which it may be originally in contact with the surface. The organic liquid condenses as a film and flows from the surface as a film. The water forms drops on the surface of the organic film and flows from the surface as a series of drops.

Flow type 2 - The converse of flow type 1, water forming the continuous film.

Flow type 3 (Channelling) - Some areas of the condenser surface are wet by the organic liquid; the remainder is wet by water. Both liquids form films over the area they wet and flow from these areas as films. Where there is an organic film, a portion of condensing water forms drops on its surface and flows from it in discrete drops to join the adjacent film of water at the boundary of the two films. Organic

liquid condenses on the water film in the same manner, and joins its adjacent film.

Flow type 4 (Double dropwise) - Neither liquid wets the condenser surface; dropwise condensation of both components occurs.

Flow type 5 - An intermediate between flow types 1 and 3. The organic liquid forms a continuous film on the condenser surface with small drops of water on its outer surface, much as in case 1, but at some point the surface is wet by isolated large drops of water which cling while the organic film flows over them. These drops finally become detached and join other water drops on the outside of the film, or they become large enough to be forced slowly down the condenser surface as a result of the flow of film past them.

Flow type 6 - The converse of flow type 5, with water as the film (p. 3).

The correlations of Hazelton and Baker are not dimensionally consistent, and should be used only with the English (U.S. customary) system of units. Their theoretical equation was:

$$h = 0.943 \left[\frac{K_1 \rho_1 (a\lambda_1 + b\lambda_2)g}{\mu_1 La \Delta t_f} \right]^{1/4} \quad (2.6)$$

and the correlations presented are,

$$h = 79 \left[\frac{a\lambda_1 + b\lambda_2}{aL} \right]^{1/4} \quad (2.7)$$

for vertical tubes, and

$$h = 61 \left[\frac{a\lambda_1 + b\lambda_2}{aD} \right]^{1/4} \quad (2.8)$$

for horizontal tubes.

where:

L = length of the tube in ft,

D = diameter of the tube in ft,

K = thermal conductivity in Btu/hr-ft-deg F

ρ = density in lb/ft³,

g = gravitational acceleration in ft/hr²,

μ = viscosity in lb/ft-hr,

Δt_f = film temperature difference in deg F,

a = weight percent of component 1 (organic) in the condensate, and

b = weight percent of component 2 (aqueous) in the condensate.

$= 100 - a$

Cooper et al. (12) have presented data on isopropyl alcohol-ethyl acetate eutectic mixtures. It was reported that the heat transfer coefficients were higher for the eutectic than those obtained for pure components. They also present data on butyl acetate-steam mixture. However, in this case, the heat transfer coefficients were found to be of intermediate values compared to the two pure component condensing coefficients. Bernhardt (6) has pointed out that the butyl acetate used by Cooper et al. was only 91 percent pure, and hence, the results are of questionable value. A decreasing trend in the coefficient was reported with increasing film temperature drop.

Edwards et al. (13) condensed styrene-steam and butadiene-steam mixtures on the inside of a vertical tube. They used eutectic compositions and found that the condensing coefficients for butadiene-steam mixture matched quite closely with the McAdams equation. McAdams equation gives 20 percent higher values than Nusselt's theory. However, the data on styrene did not agree with the theoretical predictions and they recommended a correlation to be used for that system only. In the McAdams equation, they used physical properties and value of surface loading of the pure organic component only.

Tobias and Stoppel (29) studied various systems and initially tried to fit the data on the basis of the Hazelton-Baker equation. However, being unsuccessful, they developed their own equation. This equation, given below, is a modification of the Hazelton-Baker equation.

$$h = \frac{h_H}{1 - \frac{1}{545} \left[\left(\frac{\Delta\gamma^3 \Delta\rho}{\mu_a g} \right) \left(\frac{M_a \rho_b K_b}{M_b \rho_a K_a} \right)^{1/2} \right]^{0.21}} \quad (2.9)$$

where:

h_H = coefficient given by Hazelton-Baker equation,

M_a = weight rate of condensation of the organic phase,

M_b = weight rate of condensation of water,

$\Delta\rho = |\rho_a - \rho_b|$

$\Delta\gamma$ = the difference in surface tension of water and the organic at the eutectic temperature,

μ_a = viscosity of organic phase,

ρ_a = density of organic phase,

ρ_b = density of aqueous phase,

K_a = thermal conductivity of organic phase, and

K_b = thermal conductivity of aqueous phase.

The equation shows considerable deviation in some cases and an explanation is given by Tobias and Stoppel (29). The anomalies resulting from the equation were anticipated. If water condenses alone, the numerator of the equation becomes infinite and if the organic component condenses alone, the denominator becomes negatively infinite. Also, the denominator becomes zero if:

$$\left[\left(\frac{\Delta\gamma^3 \Delta\rho}{\mu_a g} \right) \left(\frac{M_a \rho_b K_b}{M_b \rho_b K_a} \right)^{1/2} \right]^{0.21} = 545$$

This is possible at very low percentages of water in the condensate.

Hence, a range of 8 to 98 percent water by weight was recommended.

Investigation Using Other Geometries

Akers and Turner (1) used various mixtures including non-eutectics on a vertical "cold finger" of brass, 2.5 inches in diameter and 3 inches long. Their data are within 2 percent of that for the corresponding eutectic compositions most of the time. They have noted a number of interesting observations which confirm that the mechanism of two phase condensation is quite complex and is not yet fully understood.

Akers and Turner introduced the Harkins and Feldman (14) concept of spreading coefficients. For two liquids A and B, the spreading coefficients S_{BA} for A spreading over B and S_{AB} for spreading B over A are defined as:

$$S_{AB} = \gamma_B - \gamma_A - \gamma_{AB} \quad (2.10)$$

and

$$S_{BA} = \gamma_A - \gamma_B - \gamma_{AB} \quad (2.11)$$

where:

γ_A = surface tension of A,

γ_B = surface tension of B, and

γ_{AB} = interfacial tension between liquids A and B

If the spreading coefficient S_{BA} is positive, then B will spread over a drop of A and form a film over it. For $S_{BA} < 0$, liquid A

will form drops and liquid B will form a film around it, the drops of A standing exposed to the vapor. Akers and Turner state that, though it is not possible to predict the mechanism of two phase condensation accurately, the spreading coefficients are certainly indicative.

For predicting the heat transfer coefficients, they have developed two equations. For the film-drop and the film-lens mechanism, they use the Nusselt equation,

$$h \left(\frac{\mu^2}{K^3 \rho^2 g} \right)^{1/3} = 1.47 \left(\frac{4\Gamma}{\mu} \right)^{-1/3} \quad (2.12)$$

The viscosity of the surface-wetting liquid is used. The density is averaged based upon weight percent, and the thermal conductivity of the condensate is averaged based upon volume percent. All their data fit within 30 percent of the predicted values.

For channeling flow, they have found that the data closely parallel, but are 20 percent below those predicted by the Kirkbride equation. Hence, they have recommended the use of:

$$h = 0.8 \left(\frac{a\lambda_a h_a + b\lambda_b h_b}{a\lambda_a b\lambda_b} \right) \quad (2.13)$$

where:

a = heat load on component 1 (organic),

b = heat load on component 2 (aqueous),

h_a = coefficient for organic phase calculated using the Nusselt equation, and

h_b = coefficient for aqueous phase calculated using the Nusselt equation.

The work of Bernhardt et al. (7) is unique in the matter of visual observations and experimental techniques. A vertical gold-plated copper plate was used as the condensing surface. Detailed motion pictures of the mechanism of condensation were taken. An electrical probe assembly and a dye technique were used independently to prove that, in the film-drop and film-lens mechanism, the film was always made of the organic phase and the discrete drops were of water. Before this study, it was only guessed that the film would be organic. The motion pictures show that the large standing drops of water as well as the surrounding organic liquid film were both in contact with the metal surface, and also exposed to the vapor. Hence the configuration is non-equilibrium with four phases, namely, solid-liquid-liquid-vapor. Bernhardt et al. state that no correct theoretical treatment is available, and hence empiricism is necessary for predicting heat transfer coefficients. Using a shared surface model, they have recommended a very simple expression. This equation calculates an average of the pure component heat transfer coefficient based on the volume fraction of each phase in the condensate. The equation is written as:

$$h = h_1 v_1 + h_2 v_2 \quad (2.14)$$

where:

h_1 = coefficient for organic phase calculated by Nusselt equation, assuming only organic is present.

h_2 = coefficient for aqueous phase calculated by Nusselt equation, assuming only water is present.

v_1 = volume fraction of the organic phase in the condensate,

v_2 = volume fraction of the aqueous phase in the condensate.

The equation fits most of the data within 20 percent.

Boyes and Ponters (8) studied the behavior of organic and water phases in contact with a copper as well as a PTFE surface. The experimental conditions were static. There was no continuous heat removal from the condensing surface and the condensate was not drained out. Using needles, drops of liquids were introduced on the surface. They found that the surface force as well as the bouyancy force plays an important part in determining the hydrodynamic behavior.

Summary

There are many questions still to be answered as to the effect of certain variables which may be expected to influence the condensation of steam-organic mixtures, film temperature difference being one of the very important ones. Another parameter which does not seem to be considered by most workers is the density ratio of the two components. This is surprising since one would expect this to be of considerable importance, particularly on horizontal tubes where gravity is likely to play an important role in drop behavior. That is, different heat transfer effects would be expected for drops which touched the metal surface as opposed to those which float on the film.

The mechanisms of condensation as described by Hazelton and Baker are given above. In practice, the only mechanisms which have been observed are those of types 1, 3 and 5. The types which have water as the continuous film and organic as the drops (type 2 and 6) are not likely to be realized with any common organic components. The double dropwise mode (type 5) might be possible with water and selected

organics condensing on a low energy surfaces such as PTFE, although this has not been achieved in practice.

Very little work has been done on the condensation of organic-organic mixtures, this perhaps being due to the greater commercial interest in the organic-steam mixtures. The only reported data of this kind are those of Akers and Turner on heptane-methanol mixtures. They describe the mechanism as being film-lens type, but do not state which component formed the film and which formed the lens. Equation (2.12) was used to correlate the data obtained, and was accurate within 25 percent.

Some other effects have not been studied by any of the above investigators. There is no published work on the effect of noncondensible gases on the condensation process. This is not at all surprising since the mechanism for the case of pure component mixtures itself is not clearly understood, and the introduction of the noncondensible gas would complicate the mechanism further.

The only work in which high vapor velocities have been used was that of Yusofova and Neikducht, this being for a petroleum fraction and steam. No data exist on a single component organic condensing with steam. Hence, the effects of vapor shear are unknown.

No data are available for the condensation of immiscible mixtures on tube banks, nor has there been any work published on the in-tube condensation of binary mixtures. Obviously, further work is required in all the above areas before a fuller understanding of the problem can be attained.

CHAPTER III

APPARATUS

Introduction

The apparatus was designed and assembled with the goal of obtaining qualitative (visual) as well as quantitative data. However, the main objective was to locate the problems that would be encountered in this type of experiment and find ways to eliminate them. The apparatus consists of several components and can be broadly subdivided into four sections: the vapor side system, the cooling water system, temperature measurement and photography. A schematic flow diagram of the process is given in Figure 2.

The boiling equipment consists of a 5 liter (1.32 gal) flask, heated by a heating mantle. The vapors of the single component or the boiling mixture are carried out through a 1/2 in x 20 BWG, 316 stainless steel (henceforth referred to as 316SS) tube. The vapor is passed through a pipe tee, where the liquid droplets separate and return back to the flask. The vapor is then let to the condensation cell from its top. The condensate from the test surface is removed by a 1/4 in x 20 BWG, 316SS tube. The condensate either may be led outside for a measurement, or returned to the flask. The uncondensed vapor along with the condensate from the cell wall is taken out at the bottom of the cell through a 1/2 in x 20 BWG, 316SS tube and led to the auxiliary condenser.

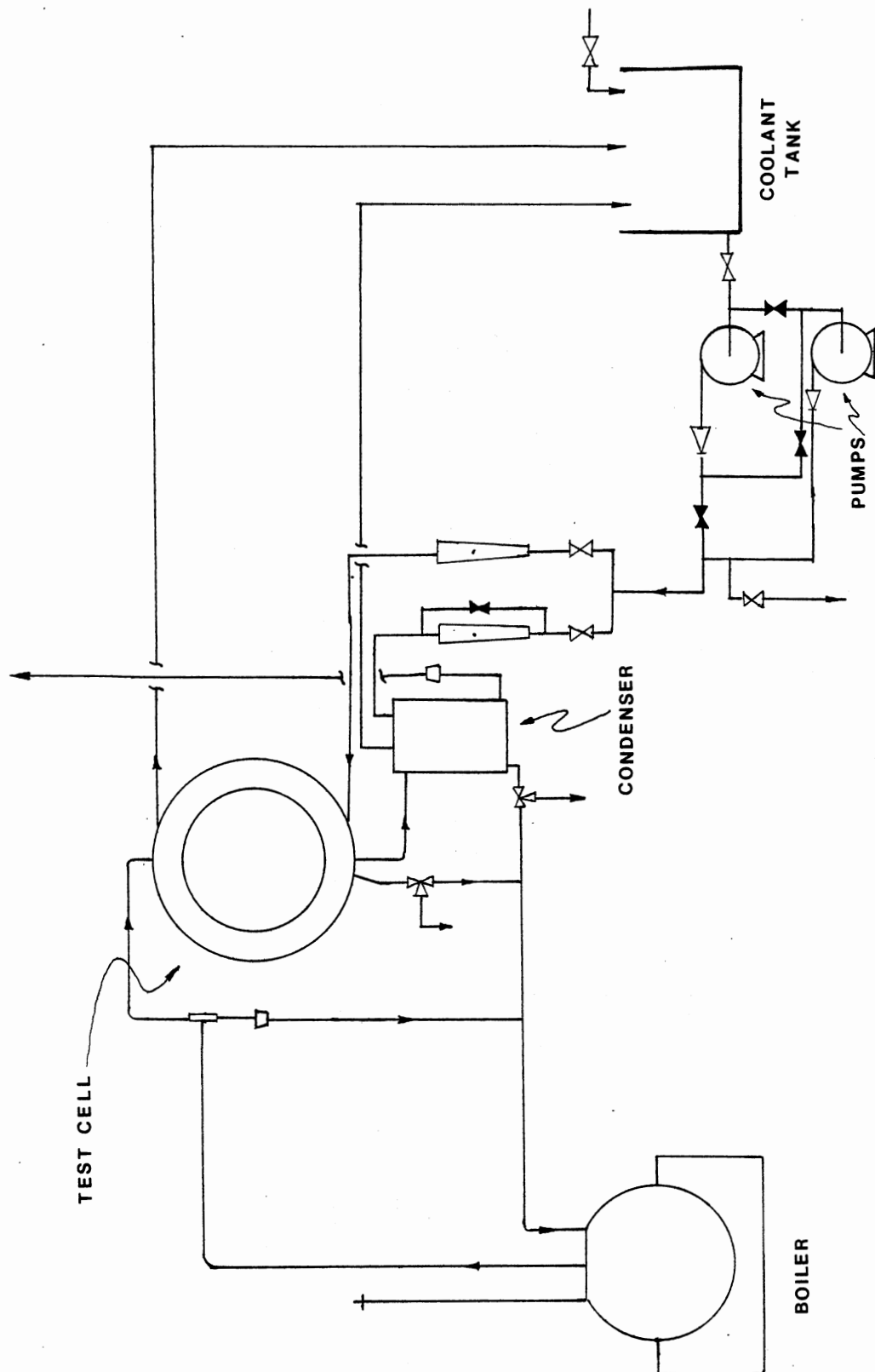


Figure 2. Schematic Flow Diagram

The condenser has approximately 0.62 ft^2 (0.0558 m^2) of condensing surface area and is able to condense all the vapor coming to it. The condensate is led out through a $1/4 \text{ in.} \times 20 \text{ BWG}$, 316SS tube from the bottom and may be taken out for collection and measurement, or returned to the boiling flask. A $1/2 \text{ in.} \times 20 \text{ BWG}$, 316SS tube is connected to condenser and led to the vent at a substantially higher level.

The cooling water is taken from a feed tank filled with tap water. Two centrifugal pumps are used. They are connected in such a way that they may be used either in series, in parallel, or independently of each other. The water flow is divided, with one branch for the test cell and the other for the auxillary condenser. Two rotameters were used to measure the individual flow rates. The coolant flow out of the cell and the condenser were returned independently to the feed tank. A $1/4 \text{ in.} \times 20 \text{ BWG}$, 316SS tube was used throughout for water. A detailed description of the components is given below.

Vapor Side System

Vapor Generation

The vapor generator consists of a 5 liter (3.2 gal), pyrex glass, round-bottom, three-necked flask. All three openings are closed by stoppers. The central, bigger neck is used as the vapor outlet. The stopper is drilled with a $1/2 \text{ in}$ hole and a $1/2 \text{ in.} \times 20 \text{ BWG}$, 316SS tube is forced through it. This tube is connected to another 316SS tube, using a $1/2 \text{ in}$ brass union joint.

In one of the smaller necks, a $3/8 \text{ in}$ glass tube is inserted which extends to the bottom of the flask. This tube is approximately 3 feet

(90 cm) long and can be closed at the top by a #0 stopper. This tube serves as a feed line to the flask when it is in operation. Using a glass funnel, additional amounts of liquids are added to the flask without stopping the boiling or shutting off the experiment. When open at the top, this tube serves as a barometric leg to indicate the excess pressure maintained in the flask.

The stopper in the third neck is drilled with a 1/4 in. hole and a 1/4 in.x 20 BWG, 316SS tube is forced in. The tube extends to the bottom of the flask and serves as a condensate return line. The other end of this tube is connected to the three condensate return lines through a union cross. During operation the lower ends of the liquid return line and the glass tube are always immersed in liquid.

Heat is supplied to the flask with a Glas-Col^R heating mantle, STM 1300. It has two separate heating circuits with a 700W/110V rating each. Power is supplied to these using separate Variacs.^R The upper circuit is switched on only after the lower circuit is at full power. Initially, a 600W/100V Glas-Col^R heating mantle 0-414 was used. It was found that for steam generation, the amount of vapor generated was not enough to meet the requirements of the cell.

Condensation Cell

The condensation cell consists of three major components: The vapor chamber, the coolant chamber, and the test surface. A drawing of the assembled cell is given in Figure 3.

The vapor chamber is made of brass. A cylindrical ring 6 1/4 in. (159mm) diameter and 1 in. (25.4mm) wide, is fitted with two flanges at the two ends. These two flanges as well as the coolant chamber

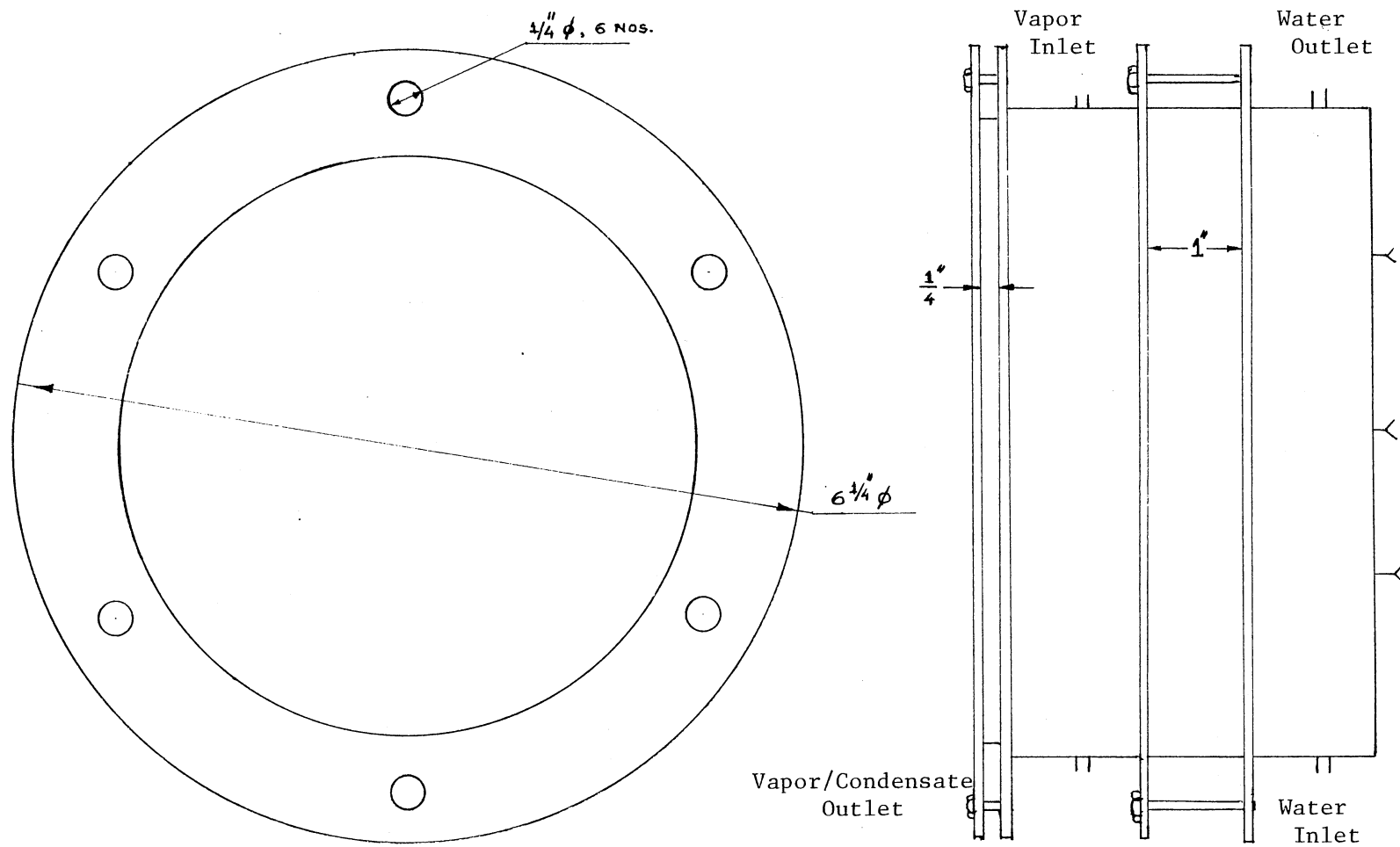


Figure 3. Assembled Test Cell

flange are 5 1/2 in. (140mm) i.d., 8 in. (203mm) o.d., and 3/8 in. (9.5mm) thick. The vapor chamber flanges have grooves for one O ring gasket each. On the front side, a 6 in. (152mm) diameter, 1/4 in. (0.64mm) thick glass plate is placed and secured in place by using another flange. The purpose of the glass is to allow visual observation and to photograph the test surface during the experiments. The vapor chamber has 1/2 in. pipe threads at the top for connection to the vapor line. At the bottom is a 1/2 in. pipe-threaded outlet. This is connected to the auxiliary condenser. It has a bypass line just below the cell, which can be used as a drain. The drain is kept closed during operation and may be used for purging. On the side of the chamber, at 105°, a hole was drilled and tapped with 1/4 in. pipe threads. This was used for fitting a thermocouple in the vapor space.

The coolant chamber is also made from a 6 1/4 in. (159mm) diameter brass ring, 1 in. (25.4mm) wide. The back is closed off with a 6 1/4 in. (159mm) brass plate. On this back plate, six holes are drilled and tapped with 1/4 in. pipe threads. These are used to pass the thermocouples connected to the copper plate. Each thermocouple wire is passed through a Teflon^R plug. The plugs are fitted in place to seal off the holes. On the other side of the coolant chamber, a flange is welded. It has six holes tapped with 1/8 in. pipe threads. This flange is bolted to the back flange of the vapor chamber, holding the copper plate between the two. The plate separates the two chambers and forms the condensation surface. The coolant chamber has two 1/4 in. threaded holes for water flow. The one at the bottom serves as inlet and the one at the top is the outlet.

The condensate surface is machined from a 1 in. (2.54mm) thick copper plate, 6 1/4 in. (1.59mm) in diameter. A detailed sketch of the plate is given in Figure 4. From the front side, 3/4 in. (19mm) of the plate thickness is carved out. The 5 in. (127mm) diameter indented surface acts as the test surface. The machining is done at an angle. This separates the condensate collected off the test surface from the condensate formed on the walls of the vapor chamber. The pit formed at the bottom of the surface holds the condensate from the test surface in a small pool. A 5/32 in. (4mm) diameter hole is made at the bottom of the pit touching the test surface. A 1/4 in. copper tube is connected there for drawing out the condensate. The condensate line is connected to a two-way valve. This valve may be fully blocked, or connected to the measurement outlet, or to the condensate return line. From the back of the plate six holes are drilled to place the thermocouples. These are three identical pairs situated along the height of the plate. Of each pair, one hole is 1/8 in. (3.175mm) deep and the other goes up to 30/1000 in. (0.762mm) from the front surface. One thermocouple is placed in each of the holes and then filled with liquid solder.

Auxiliary Condenser

The auxiliary condenser is designed to condense all the vapor that may come to it from the cell. During the several runs, the heat load on the test cell is varied, and hence the heat load on the condenser also varies. The condenser consists of a cylindrical shell of copper, 5 in. (127mm) diameter and 10 in. (254mm) long. The shell is closed on both the sides and supported vertically. A copper coil is suspended

All Dimensions in inches

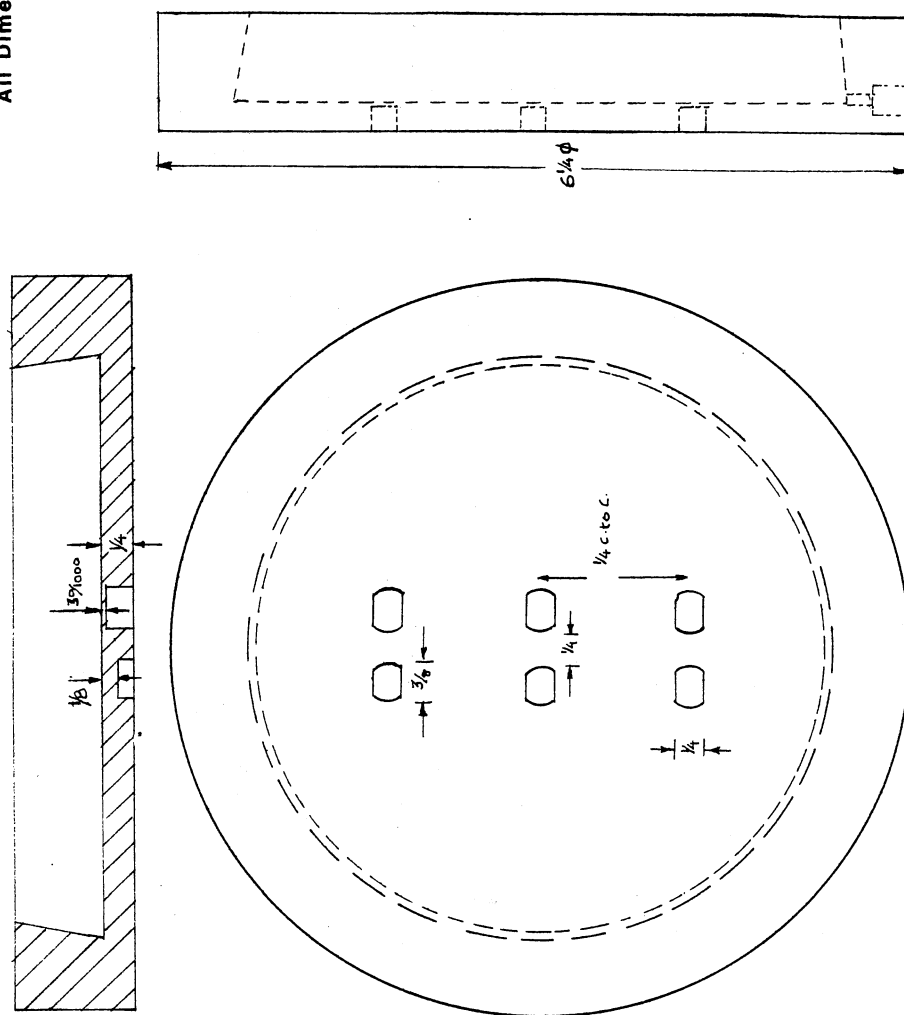


Figure 4. Sketch of the Plate

from the top end. The coil is made from a 1/4 in. copper tube, is 8 inches (203mm) long and has a 3 in. (76mm) diameter, and has 1.5 turns per in. of length. An effective outside surface area of 0.62 ft^2 (0.0558 m^2) is obtained. The vapor-liquid mixture comes in from the side openings at the top. The condensate is withdrawn from the bottom and passes through a 2-way valve. The valve may be opened to the condensate return line, or to the outside line for measurement and withdrawal from the system. Another opening is provided on the shell side of the condenser. This is connected to a tube open in the vent. The vent opens approximately 4 1/2 ft (115mm) above the condenser and 10 ft (3 m) of tube length away. In case of failure in the auxiliary condenser, the uncondensed vapors will be safely purged out through the vent. The vent also acts as a purge for the noncondensibles during normal operation. A sketch of the condenser is shown in Figure 5.

Cooling System

Pumps

Initially, only one pump was used to supply cooling water to both the condensation cell and auxiliary condenser. The pump was an Eastern MD15T with a rating of 4.76 gpm (18 lit / min) and 9 ft (2.7 m) head. The pressure drop through the system was much greater, and the flow rate dropped to a very small value. Another pump was added to the piping. This was an Eastern D-10 with 2.64 gmp (10 lit/min) rating. This pump was connected in such a way that it could be operated in series or in parallel with the first pump. Also, it was possible to

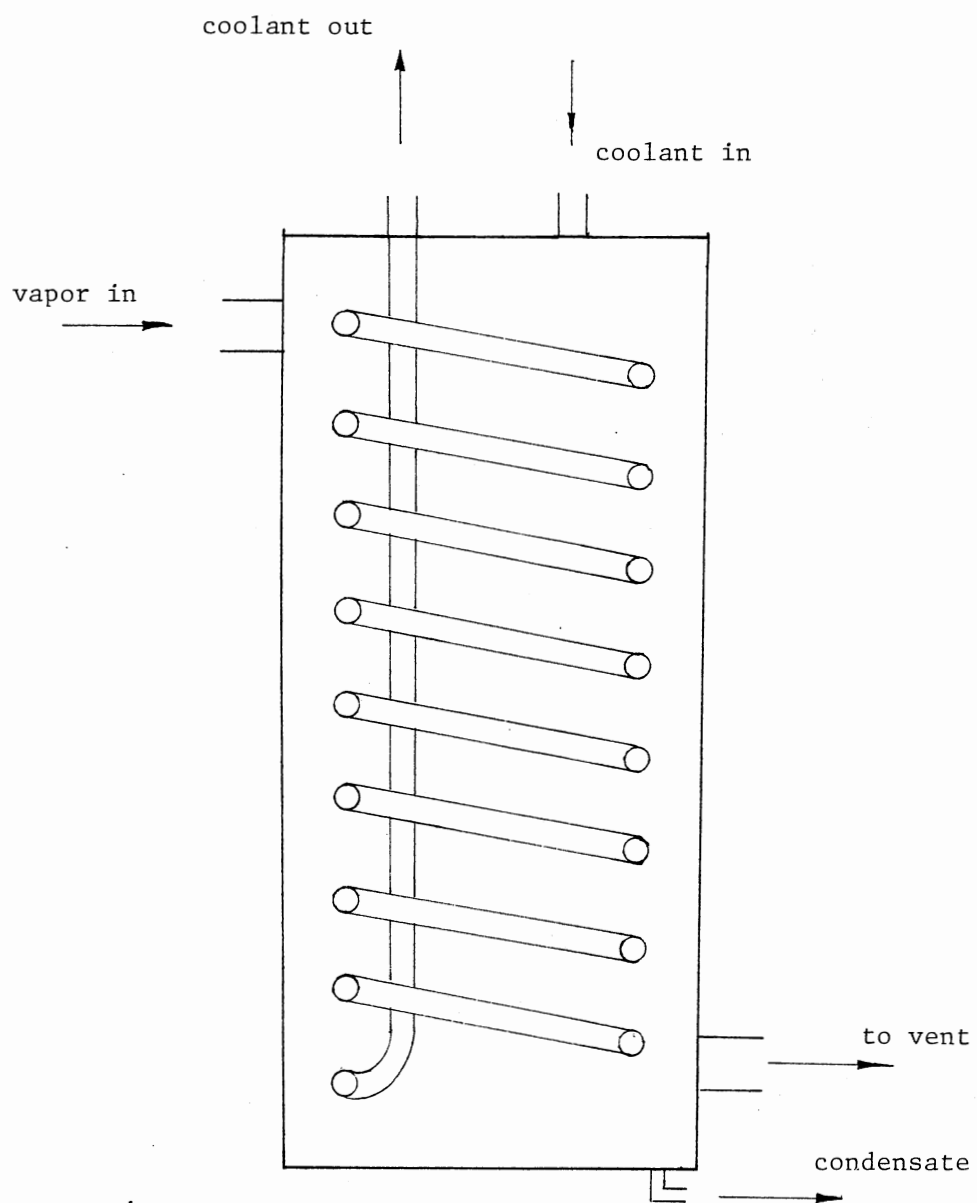


Figure 5. Auxiliary Condenser .

operate either pump independently of the other. This gave a wide range of control over the flow rate. A schematic diagram is shown in Figure 2.

Rotameters

For measurement of water flow rate to the test cell and the condenser, two separate rotameters were used. For the cell, a Fischer and Porter FP-1/2-35-G-10/35 rotameter tube with a range of 0.2 to 2 gpm (0.757 to 7.57 lit/min) was used. The rotameter was specially made and precalibrated. The calibrations were checked and found to be accurate. To measure the flow rate to the condenser, a Fischer and Porter FP-1/4-20-G-5/84 rotameter was used. It was found that the upper limit on the measurement was too small. Hence, a 1/4 in tube with a toggle valve was connected parallel to the rotameter. The range was nearly doubled with the parallel flow. The rotameter was recalibrated. A number of flow measurements were done at various readings on the meter. A seventh order Lagrangian polynomial was used to express the flow rate as a smooth function of the rotameter reading. The readings were taken using a spherical stainless steel float. A calibration chart is in Appendix C.

Piping System

For the circulation of cooling water, 1/4 in x 20 BWG, 316SS tubes were used throughout. All the tube fittings used were of brass. A controlled drain was provided downstream from the pumps. This was used to remove hot water from the cooling system. Adding controlled amounts of cold water to the feed tank, the coolant temperature could

be roughly controlled, or brought down to a desired level.

Temperature Measurement

The main component in the temperature measurement was the Leeds and Northrup K-5, Series 7555 potentiometer. The calibration and measurement instructions were followed from the K-5 potentiometer User's Manual (20). The medium range settings were used through out with a range of 0 to 0.161105 volts. The limit of error was \pm (0.005 percent of the reading + 0.3 microvolts). The potentiometer uses a standard cell of 1.01930 volts. Copper-Constantan (type T) thermocouples were used as the sensing elements. The thermocouple wire was obtained from Omega Engineering and the beads were made using a bead welding machine. All the thermocouples were connected to a Doric Selector Switch Box. Two thermocouples were always immersed in a ice-water bath. The connections were made inside the selector in such a way that the electromotive force measured was always a differential. For measuring actual temperatures, this differential was with respect to the ice-water bath temperature. It was also possible to measure the differential between a pair of thermocouples connected to the test plate. Of this pair, one thermocouple was very near the front surface and the other was half way through the plate thickness.

In the initial runs, because of the low values of the coefficients obtained, it was suspected that the thermocouples were not in good contact with the copper plate. It was found by measuring the electrical resistances that the thermocouple beads were not touching the copper plate. Possibly, some of the adhesive material had slipped between

the thermocouple tip and the plate surface. The thermocouples were removed and reattached. It was then found that the thermocouples were in physical contact with the surface. This created a sudden drop in the temperature readings. The voltmeter was internally connected in such a way that the negative leg of the thermocouple loop was grounded. The link between the negative port and the ground port was opened. With this, the thermocouple readings were back to normal.

Photography

In order to make visual observations and obtain photographs of the condensation patterns, it was necessary to have a fog-free window. A search was made to procure electrically conducting glass similar to that of Bernhardt. However, finally a simple 1/8 in (3.18mm) thick pyrex glass was used. When glass was exposed to the cold surroundings, vapor condenses and fogs the inner surface. Initially, attempts were made to heat the glass with a hot air blower. At this time runs were made with pure steam and the blower was found to be inadequate. Infra-red lamps were then used to heat the glass. Two reflector lamps of 250W/110V each were used. The voltage to these was controlled by a variac and the power kept just adequate to keep the glass clear. This was found to be a fairly successful method to keep the glass clear. For providing natural (tungsten - visible range) light, two flood lights were used. They were 250W/110V and 150W/110V, respectively.

A Nikon-F 35 mm camera was used to obtain the still photographs. Three extension rings, namely, K2, K3, and K4 were used. With these the camera could be focused at about 6 inches (15 cm) from the object.

The black-and-white film used was Kodak Plus-X pan film 125 ASA. A color film, Kodacolor II, 100 ASA was initially used to obtain photographs of steam condensing in a dropwise manner. Photographs were taken mainly at a speed of $1/125$ th of a second. The aperture size (f/stop) was kept at 4.0.

Motion photography was done using a Bolex 16 mm camera. The film used was black and white Kodak Plus-X, reversal type. Two different lenses were used. The first was 75 mm focal length with 10 mm extension ring, for closeup pictures. The other was a 50 mm focal length used for a view about 2 ft (60 cm) away from the test surface. The camera was run using a motor drive. The filming was done at a standard speed of 24 frames per second throughout.

CHAPTER IV

EXPERIMENTAL PROCEDURE

After assembling the equipment, the entire piping system was flooded with water to check for leaks, if any. Flooding was done separately for the vapor and coolant paths. This ensured that the two were isolated from each other.

When the test surface was fresh, it had very small marks of machining. The circular pattern of a lathe tool was visible. However, no polishing was done. These marks were not visible to the naked eye after a working time (in condensation service) of approximately 15 hours. Initial runs were made using steam as the condensing substance. During these runs, tests were done to check the capacity of the auxiliary condenser. The coolant supply to the test cell was cut off and all the vapor was passed to the auxiliary condenser. The condenser was able to condense all the vapor generated in the boiler. The vent line was not purging any vapor and the vent pipe was at room temperature beyond the first three inches of its length.

Approximately 25 initial runs were made to age the surface, each lasting approximately two hours. During these runs, a coating of copper oxide appeared on the surface. These runs were made primarily to overcome effects due to the freshness of the test surface.

The first step to start the experiments was to turn on the potentiometer. The User's Manual for the K-5 potentiometer (20) recommends that the readings will be sufficiently accurate after a warm-up period of 15 minutes, and very accurate after an hour. The coolant feed tank was filled approximately to three fourths of its volume by tap water. The valve to the auxiliary condenser was opened and the pumps started. The coolant flow to the test cell was shut off. The test liquid or liquid mixture was added to the boiling flask. The flask was filled a little over half of its volume, corresponding to a liquid level slightly above the upper edge of the heating mantle. The heaters were then turned on. The infrared floodlights were also turned on to heat the front glass of the test cell. The voltage to these was regulated at 75 volts.

After the boiling started, some vapor condensed in the test cell and the rest went to the auxiliary condenser. A period of 20 minutes was allowed to elapse during which more and more vapor passed on to the condenser without condensing in the test cell. This vapor was expected to drive away all the air present in the cell initially.

The coolant flow to the test cell was slowly started. The temperatures, flow rates and condensing rates were noted after 20 to 25 minutes. The ice used in the ice-water bath was made from tap water and the temperature of the bath was assumed to be 32°F (0°C).

While obtaining still photographs, the infrared heaters were temporarily switched off and the tungsten visible lights were switched on. The infrared heaters were switched off in order to avoid heating of the camera. The glass would start to fog 50 to 55 seconds after turning off the infrared lamps. Hence a continuous sequence of photographs

was confined to a period less than 50 seconds.

The lenses used on the motion picture camera were of higher focal length and it was possible to photograph the test surface from a longer distance. Hence, the infrared lamps were not disturbed and white lights were temporarily turned on when the camera was running. By switching the power to the driver motor, the camera action was controlled remotely. This eliminated any vibrations as well as shaking that may occur in a hand-held, manually-triggered camera.

For shutdown, power to the boiler was shut off. All lamps, infrared and white, were shut off. The coolant flow to the cell and the condenser was opened fully. The potentiometer was switched off and the thermocouple in the ice-water bath was removed.

CHAPTER V

DATA ANALYSIS

Data on Steam

All the initial runs were made using steam as the condensing substance. Initially, when the surface was fresh, almost all the surface exhibited dropwise condensation. The pattern started to change gradually in isolated spots as the surface converted to copper oxide. Table I gives the condensing heat transfer coefficients obtained during these runs. The coefficients predicted using the Nusselt equation are also given. The detailed calculations are shown in Appendix D. The values obtained experimentally are found to be substantially lower than the predicted values. This was attributed to the presence of noncondensable gas, that is air, in the test section. Othmer (22) has shown that the presence of small amounts of noncondensables in the vapor can reduce the condensing coefficients to a fraction of what they would be otherwise. Figure 6 gives a quantitative estimate of the effect of presence of air.

When the vapor enters the test section, the cross-sectional area for flow increases suddenly. Also the rate of vapor delivery to the test section is not sufficiently large to allow uncondensed vapor to leave the test section. Calculation of the heat load on the auxiliary

TABLE I
RESULTS FROM THE STEAM RUNS

Run #	Heat Duty Q Btu/hr	Heat Transfer Coefficient Btu/hr-ft ² -°F		
		Calculated	Experimental	
			h_1	h_5
15	2,852	2,220	597	721
16	2,728	2,315	533	513
17	2,133	2,513	802	1,194
18	2,604	2,351	384	374
19	1,116	3,118	141	143
20	1,934	2,596	292	310
21	2,852	2,281	1,030	1,394
23	2,855	2,280	889	1,118

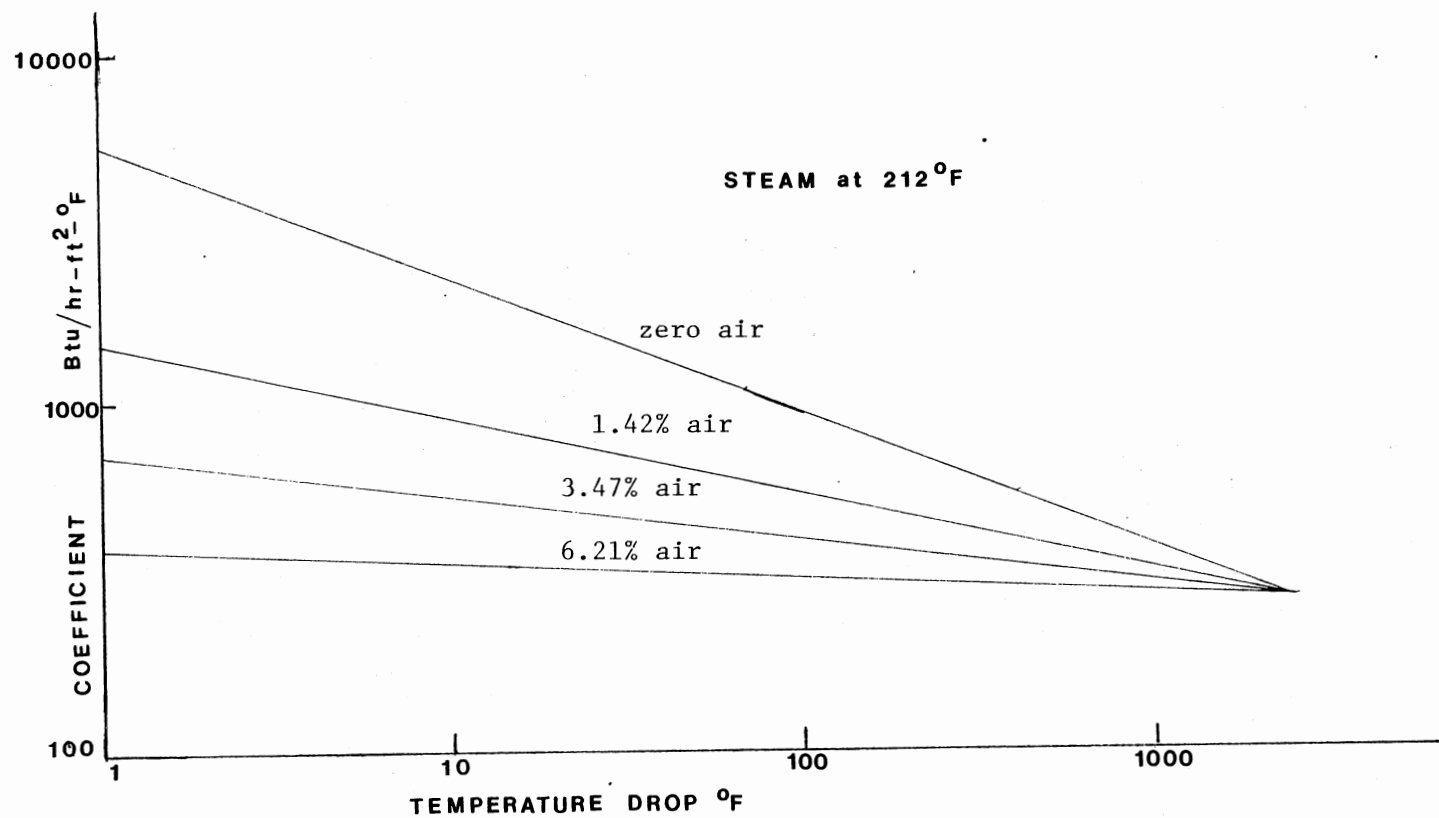


Figure 6. Effect of Noncondensables on Condensing Coefficient (Othmer (22))

condenser point this out. Almost all the steam condenses in the test cell and a negligibly small amount appears in the condenser. Consequently the air present initially in the chamber may not be removed. If the coolant flow to the cell is shut off, the vapors will pass through the cell uncondensed, driving out the air with it. However, as soon as the coolant flow to the test cell is started, all the vapor will condense on the test surface. This can result into a negative pressure gradient and air can reenter the vapor chamber.

When the coolant inlet temperature was approximately 125°F (52°C) and the flow rate reduced, substantial amounts of vapor left the test section without condensing. In these observations, the condensing coefficients obtained were 35 to 50 percent of the predicted values (1000 Btu/hr-ft²-°F, or 4900 Kcal/hr-m²-°C). This indicates approximately 2 to 3 percent air in the vapor chamber. When the coolant inlet temperature was 80°F (27°C) and the flow rate high, almost all the vapor condensed in the test cell. The condensing coefficients obtained were then 10 to 20 percent of the predictions (200 Btu/hr-ft²-°F, or 1000 Kcal/hr-m²-°C), indicating 5 to 8 percent air in the vapor space of the test cell.

The two solutions to the problem of noncondensables are to avoid a sudden increase in the flow cross-section for the vapor and increasing the fraction of vapor leaving the test section uncondensed.

Data on Toluene-Water System

The latent heat of evaporation of a eutectic mixture of toluene and water is only 20 percent that of pure water. Hence, with the same

amount of heat input into the boiler, the rate of vapor generation is much greater and the problem of noncondensables seems to be overcome.

Data were taken by varying the inlet temperature and the flowrate of coolant to the test cell. Table II gives the condensing coefficients obtained at the three different locations on the test surface. Figure 7 is a plot of condensing coefficients as a function of film temperature difference. Regression analysis of the data resulted in the proportionality:

$$h \propto (\Delta t_f)^{-0.4}$$

The detailed calculations are shown in Appendix E. Temperature was measured at two depths inside the test plate and by linear extrapolation the surface temperature was estimated. The vapor temperature was measured using a separate thermocouple.

Low inlet temperature and high flow rate of the coolant accompanied by reduced vapor generation rate resulted in film temperature differences of the order of 50°F (28°C). The condensing coefficients observed in these cases deviated substantially from the values predicted by Bernhardt's equation. The problem of noncondensables may exist in these runs due to the reduced vapor generation rate. Further, Bernhardt's equation is not applicable to the double dropwise condensing regime which was observed during these runs. Figure 8 is a comparison of the experimental data with the predictions using Bernhardt's equation (2.14). It can be seen that the data agree well with the predictions in the upper portion of the observed range.

TABLE II
RESULTS FROM TOLUENE-WATER RUNS

Run#	Heat Load Btu/hr-ft ²	Heat Transfer Coefficient Btu/hr-ft ²		
		Top	Middle	Bottom
24	12,113	364	308	308
25	8,507	251	240	220
26	9,564	449	389	386
27	17,957	654	640	586
28	8,464	609	717	479
29	10,392	592	602	531
30	3,683	69	88	85
31	8,289	233	235	224
32	7,373	691	833	548
33	6,024	589	680	521
34	11,944	369	342	330
35	12,511	773	817	713
36	13,693	650	688	628
37	8,948	689	701	592
38	16,902	752	666	614
39	12,113	517	445	516
40	8,954	439	429	384
41	10,272	241	234	218
42	9,286	382	448	423
43	10,795	641	791	570
44	8,687	649	698	581
45	8,579	623	659	584
46	8,587	617	600	549
47	8,420	538	560	459
48	8,289	660	665	463
49	8,289	590	631	423

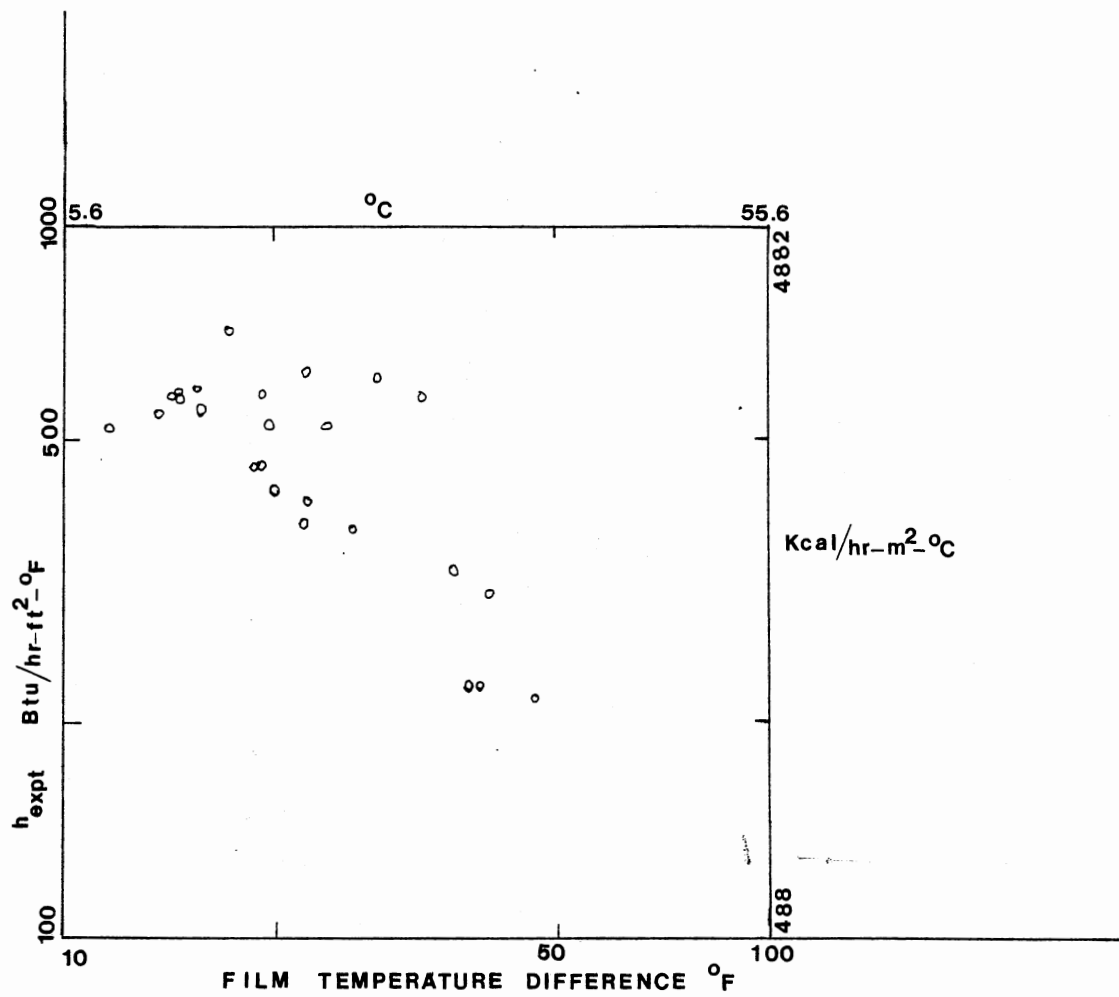


Figure 7. Heat Transfer Coefficient as a Function of the Film Temperature Difference

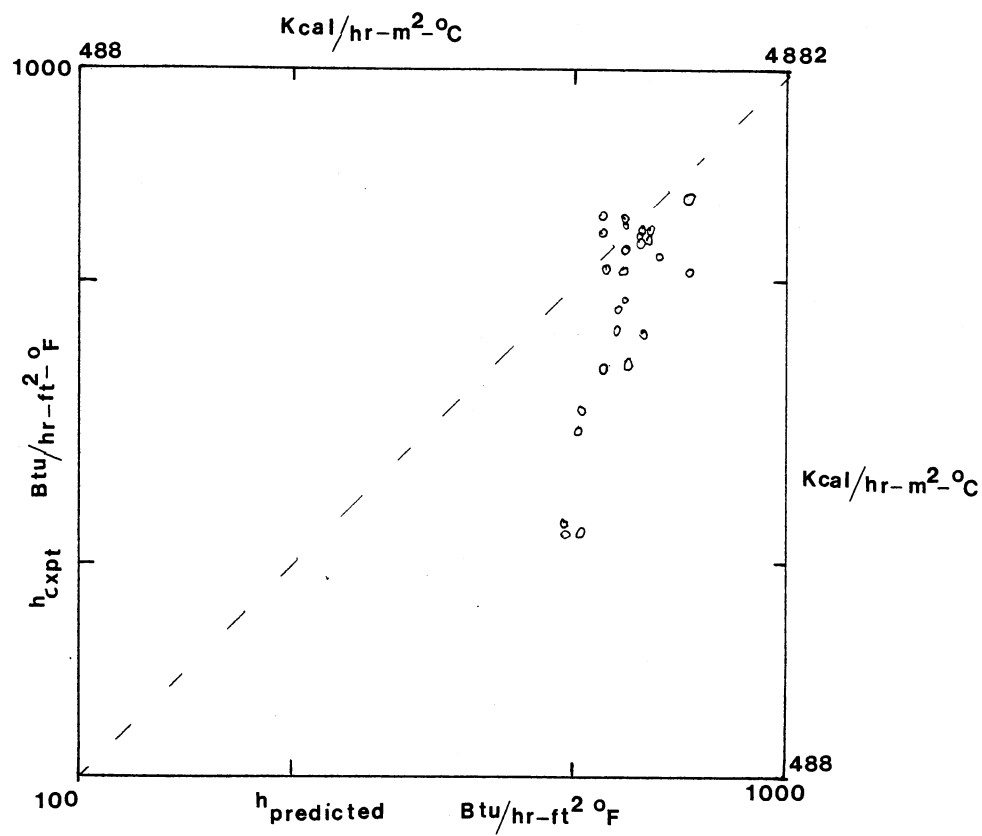


Figure 8. Comparison Between the Experimental and Predicted Values of the Heat Transfer Coefficients

Visual Observations

Through the glass window on the condensation cell, the condensation patterns were observed and photographed. Typical dropwise and filmwise patterns observed during the condensation of steam are shown in Figure 9 and Figure 10 respectively. In Figure 9 drops of various sizes are visible. Due to a predominantly smooth condensate film, the metal surface underneath the condensate film is clearly seen in Figure 10.

Figures 11 to 15 are a series of photographs taken in a sequence with a two second interval between two consecutive frames. These pictures show dropwise condensation of steam. The nucleation, growth and ultimately drainage of a drop can be observed by comparison along the sequence.

Figures 16 to 22 are pictures of two phase condensation patterns for toluene-water mixture. Figure 16 shows a predominantly double dropwise condensing pattern. The bigger drops of water drained out in the form of rivulets and the exposed surface was then occupied by new small drops of toluene. Figure 17 shows some patches of filmwise condensation. In Figure 18 the filmwise condensing pattern is predominant and isolated sections of the surface continue to exhibit dropwise condensation. The variation in the condensing pattern may be attributed to the heat load or equivalently, the ΔT_{film} . The respective heat loads corresponding to Figures 16, 17 and 18 were approximately 7,000, 12,000 and 16,000 Btu/hr-ft²-°F (34,190, 58,610, and 78,150 Kcal/hr-m²-°C).

Figures 19 to 22 are pictures taken at heat loads above 12,000 Btu/hr-ft²-°F (58,610 Kcal/hr-m²-°C). A distinct film-rivulet-drop type



Figure 9. Dropwise Condensation of Steam

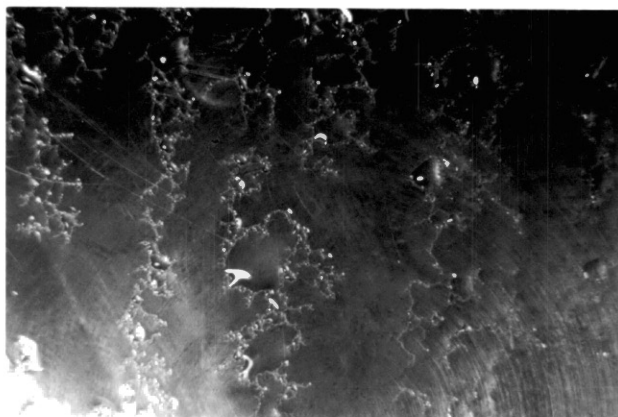


Figure 10. Filmwise Condensation of
Steam

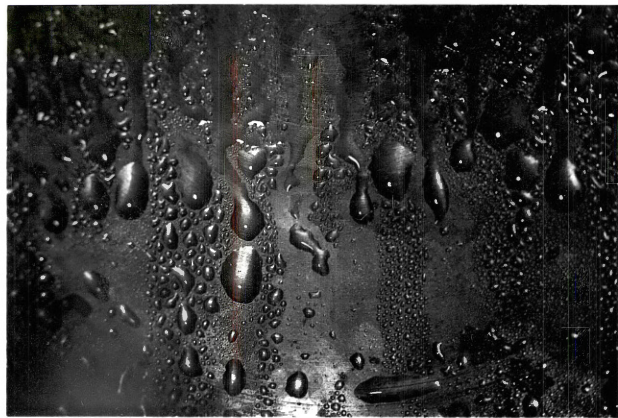


Figure 11. Dropwise Condensation Sequence
Frame 1 (steam)

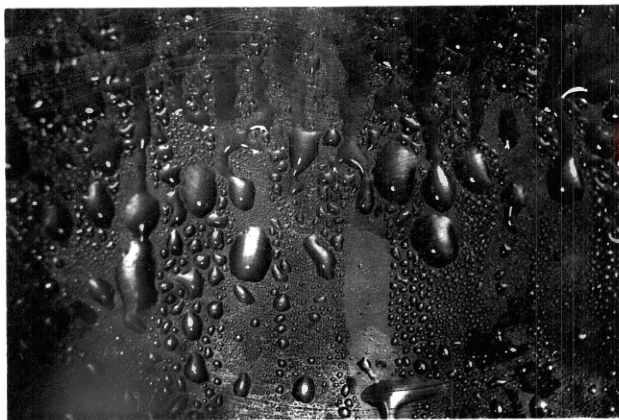


Figure 12. Dropwise Condensation Sequence
Frame 2 (steam)



Figure 13. Dropwise Condensation Sequence
Frame 3 (steam)



Figure 14. Dropwise Condensation Sequence
Frame 4 (steam)

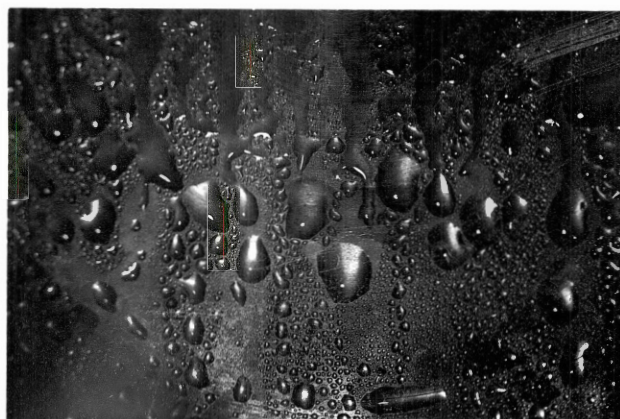


Figure 15. Dropwise Condensation Sequence
Frame 5 (steam)



Figure 16. Toluene-Water Condensation-1

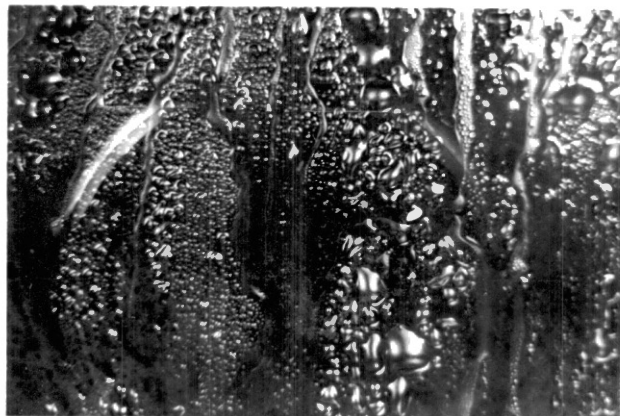


Figure 17. Toluene-Water Condensation-2

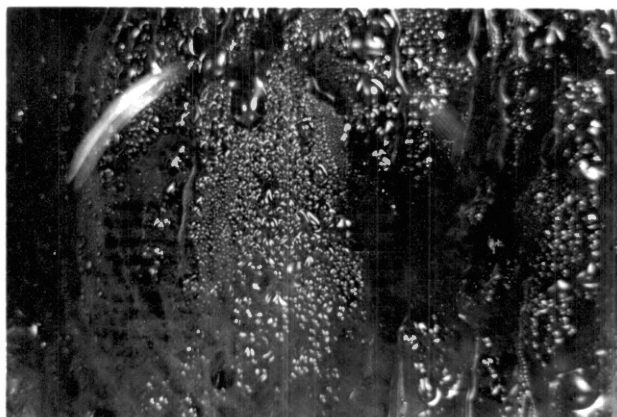


Figure 18. Toluene-Water Condensation-3

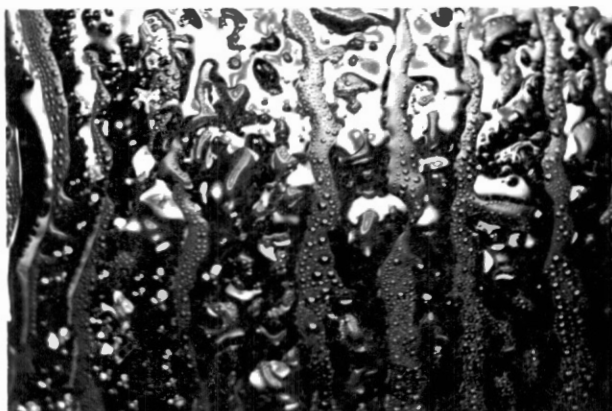


Figure 19. Toluene-Water Condensation-4



Figure 20. Toluene-Water Condensation-5



Figure 21. Toluene-Water Condensation-6

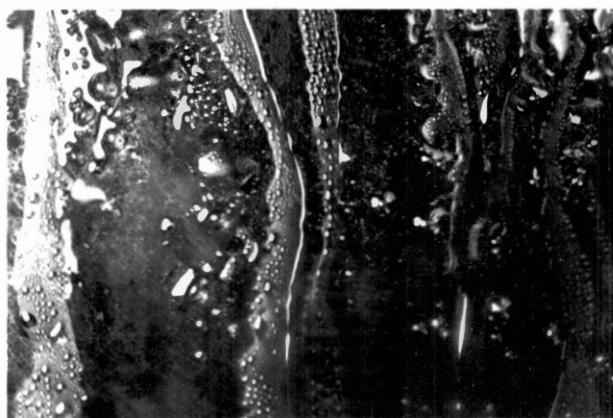


Figure 22. Toluene-Water Condensation-7

of condensation is visible. From the fractional volumes of the two phases in the condensate, it can be deduced that the film was of toluene. The rivulets were water, carrying suspended drops of toluene.

CHAPTER VI

CONCLUSIONS AND RECOMMENDATIONS

1. The presence of noncondensable gas in the condensation chamber affects the condensation substantially. Small amounts of air reduce the condensing coefficient to a small fraction of what it would be otherwise.

2. A decrease in the condensing heat transfer coefficient with an increase in the film temperature difference is found.

3. The film-rivulet-drop type and dropwise condensation patterns are observed predominantly. However, an exact correlation between the condensing patterns and the condensing coefficients is not yet available.

4. A majority of the proposed correlations in the literature are applicable to the experimental considerations used in those studies.

5. In future work, the effect of vapor shear should be studied on both the condensing patterns and heat transfer coefficients.

6. A detailed analysis of the patterns and coefficients may result in a "flow regime map" also incorporating the physical properties of the two liquids and the surface.

BIBLIOGRAPHY

1. Akers, W. W., Turner, M. M., "Condensation of Vapors of Immiscible Liquids", A.I.Ch.E.J., 8(5), 1962, p. 587.
2. Baker, E. M., Mueller, A. C., "Condensation of Vapors on a Horizontal Tube", Industrial and Engineering Chemistry, 29(9), 1937, p. 1065.
3. Baker, E. M., Mueller, A. C., "Heat Transfer Coefficients for the Condensation of Mixed Vapors of Immiscible Liquids", Industrial and Engineering Chemistry, 29(9), 1937, p. 1067.
4. Baker, E. M., Tsao, V., "Condensation of Vapors on a Horizontal Tube", Industrial and Engineering Chemistry, 32(8), 1940, p. 115.
5. Barnea, E., Mizrahi, J., "Heat Transfer Coefficients in the Condensation of a Hydrocarbon-Steam Mixture", Trans. Inst. Chem. Engrs., 50, 1972, p. 286.
6. Bernhardt, S. H., "Condensation of Immiscible Mixtures", Ph.D. Thesis, University of Illinois (1970).
7. Bernhardt, S. H., Sheridan, J. J., Westwater, J. W., "Condensation of Immiscible Mixtures", A.I.Ch.E. Symposium Series, 68(118), 1972, p. 21.
8. Boyes, A. P., Ponter, A. B., "Condensation of Immiscible Binary Systems", C.P.E. Heat Transfer Survey, 1972, p. 26.
9. Boyes, A. P., Ponter, A. B., "The Influence of Condensate Drop Size on the Dropwise Filmwise Transition for Pure Vapors", J. Chem. Eng. of Japan, 7(4), 1974, p. 314.
10. Boyko, L. D., Kruzhilin, G. N., "Heat Transfer and Hydraulic Resistance During Condensation of Steam in a Horizontal Tube in a Bundle of Tubes", Int. J. Heat Mass Transfer, 10, 1967, p. 361.
11. Colburn, A. P., "Note on the Calculation of Condensation When a Portion of Condensate Layer is in Turbulent Motion", Trans. A.I.Ch.E., 30, 1934, p. 187.

12. Cooper, A. H., Morrison, R. H., Henderson, H. E., "Heat Transfer of Condensing Organic Vapors", Industrial and Engineering Chemistry, 34(1), 1942, p. 79.
13. Edwards, D. A., Bonilla, C. F., Cichelli, M. T., "Condensation of Water, Styrene and Butadiene Vapors", Industrial and Engineering Chemistry, 40(6), 1948, p. 1105.
14. Harkins, W. D., Feldman, A., "Films. The Spreading of Liquids and the Spreading Coefficients", J. American Chem. Soc., 44(12), 1922, p. 2665.
15. Hazelton, R., Baker, E. M., "Condensation of Vapors of Immiscible Liquids", Trans. A.I.Ch.E., 40, 1944, p. 1.
16. Jakob, M., Heat Transfer. Vol. I, New York: McGraw-Hill Book Company 1949, p. 663-667.
17. Kawasaki, J. Hayakawa, T., Fujita, S., "Condensation of Binary Mixtures of Vapors of Immiscible Liquids", Heat Transfer - Japanese Research, 1(1), 1972, p. 33.
18. Kern D. Q., Process Heat Transfer. New York: McGraw-Hill Book Company, 1950, p. 241-250.
19. Kirkbride, C. G., "Heat Transmission by Condensing Pure and Mixed Substances on Horizontal Tubes", Industrial and Engineering Chemistry, 25(12), 1933, p. 1324.
20. Leeds and Northrup, Type K-5 Potentiometer Cat. 7554 and Cat. 7555, Philadelphia, 1967.
21. Onda, K., Sada, E., Takahashi, K., "The Film Condensation of Mixed Vapor in a Vertical Column", Int. J. Heat Mass Transfer, 13, 1970, p. 1415.
22. Othmer, D. F., "The Condensation of Steam", Industrial and Engineering Chemistry, 21(6), 1929, p. 576.
23. Patterson, W. C., et al., "The Condensation of Steam and Heptane on Vertical Tubes", Trans. A.I.Ch.E., 33, 1937, p. 216.
24. Patton, E. L., Feagan, R. A. Jr., "Heat Transfer Coefficients for the Condensation of Mixed Vapors of Turpentine and Water on a Single Horizontal Tube", Industrial and Engineering Chemistry, 33(10), 1941, p. 1237.
25. Polly, G. T., Calus, W. F., "The Effect of Condensate Pattern on Heat Transfer During the Condensation of Binary Mixtures of Vapors of Immiscible Liquids", Sixth International Heat Transfer Conference, Toronto, Vol. 2, 1978, p. 471.

26. Solov, V. S., Danilov, O. L., "The Condensation of Binary Mixtures of the Vapors of Immiscible Liquids on Non-Isothermal Surfaces", International Chemical Engineering, 15(1), 1975, p. 39.
27. Stepanek, J., Standart, G., "Heat Transfer During Condensation of Mixtures of Vapors of Immiscible Liquids", Collection Czechoslov Chem. Commun. 23, 1958, p. 995.
28. Sykes, J. A., Marchello, J. M., "Condensation of Immiscible Liquids on Horizontal Tubes", Industrial and Engineering Chemistry Process Design and Development, 9(1), 1970, p. 63.
29. Tobias, M., Stoppel, A. E., "Condensation of Vapors of Water and Immiscible Organic Liquids", Industrial and Engineering Chemistry Eng. Des. Proc. Der., 46(7), 1954, p. 1450.
30. Yusofova, V. D., Neikdukht, N. N., "An Investigation of the Process of Condensation of Gasoline Vapor in the Presence of Water Vapor", International Chemical Engineering, 10(3), 1970, p. 422.

APPENDIXES

APPENDIX A

ANALYSIS OF FILMWISE CONDENSATION

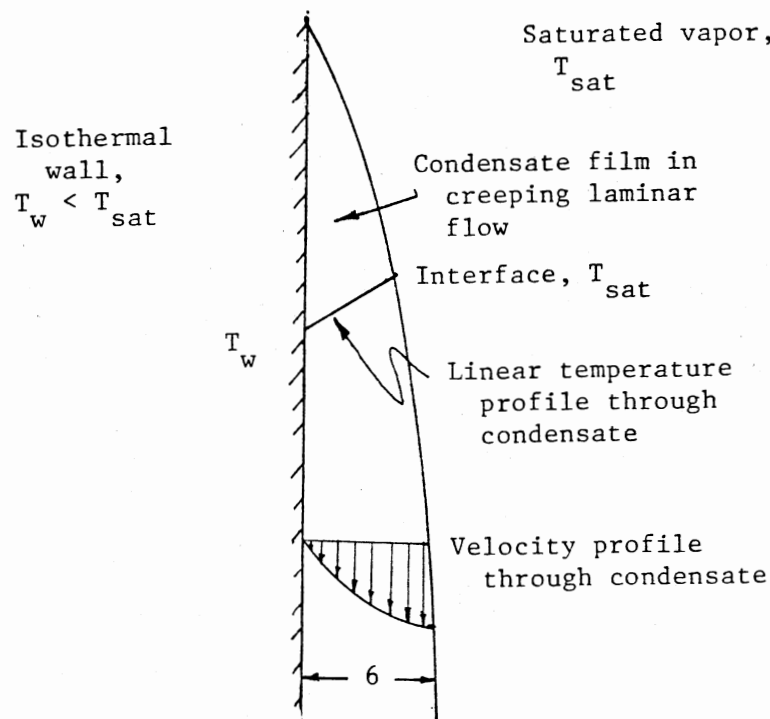


Figure 23. Filmwise Condensation

Assumptions Behind Nusselt Equation

1. Saturated vapor.
2. The liquid and the vapor have the same temperature (T_{sat}) at the interface. (No interfacial resistance.)
3. Heat is transferred by conduction only through the liquid film.
4. The temperature profile is linear through the liquid film.
5. The liquid and the solid surface are at the same temperature at their interface.
6. The solid surface is isothermal.
7. The liquid properties are not a function of temperature.
8. The vapor exerts neither shear nor normal stresses on the liquid surface.

9. The liquid has zero velocity at the liquid-solid interface (no-slip condition).
10. The sensible heat of subcooling the liquid is negligible compared to the latent heat load.

APPENDIX B

SUMMARY OF VARIOUS INVESTIGATIONS

Investigator	Test Surface	Organic Component	Condensation Pattern
--------------	--------------	-------------------	----------------------

Kirkbride (19)	Steel	Benzene Cleaners Naphtha	
----------------	-------	--------------------------------	--

Baker and Mueller (3)	Oxidized Copper	Benzene Toluene Heptane Chlorobenzene	1
--------------------------	--------------------	--	---

Baker and Tsao (4)	Oxidized Copper	Benzene Toulene Chlorobenzene Trichloro- ethylene Tetrachloro- ethylene	1, 3, 5
-----------------------	--------------------	---	---------

Patton and Feagan (24)	Oxidized Copper	Turpentine	1
---------------------------	--------------------	------------	---

Sykes and Marchello (28)	Copper	Toulene Carbontetra- chloride	
-----------------------------	--------	-------------------------------------	--

Correlation Proposed

$$h = \frac{h_1 Q_1 + h_2 Q_2}{Q_1 + Q_2}$$

$$h \left(\frac{\mu_1^2}{k_{av}^3 \rho_{av}^2} \right)^{1/3} = 1.28 \left(\frac{C_{pav} \mu_1 \rho_{av}^{0.7}}{k_{av} \lambda_{av}} \right)^{2.38} \left(\frac{Q_1}{Q} \right)^{-3.28}$$

$$\frac{h}{1 - \frac{0.0167}{D}} = \frac{500}{1 - 0.0085 V_2} + 80$$

$$h = \frac{366 D^{-1/4} (1 - \frac{0.0284}{D})}{1 - 0.0085 V_2}$$

$$h = 3000 (\Delta t)^{-0.5}$$

$$h = h_1 (1 - 0.8R) (\Delta t_f)^{0.67R}$$

and

$$h = h_1 \left(K_1 + \frac{1}{K_2 e^{\beta \Delta t_f}} \right)^{-1}$$

$$k_1 = [7.6 - 1.8(P_{r1} - P_{r2})]^{-1}$$

$$k_2 = \frac{17.3 \times 10^{-10} P_1 (1 + \frac{a \lambda_1}{b \lambda_2})}{[(Oh)_1 (\frac{\Delta Y}{Y_1})^{1/2} (\frac{\mu_1}{\mu_2}) (\frac{M_2}{M_1})]^2}$$

Investigator	Test Surface	Organic Component	Condensation Pattern	Correlation Proposed
Stepanek and Standart (27)	Copper	Benzene Toluene Dichloroethane Chlorobenzene	Assumed 1	$h = 0.725 \frac{\lambda_{av} K_1^2 \rho_1^2 g}{\mu_2 \Delta t_f D}^{1/4} \times K_3 (1 + K_4 \Delta t_f)$ $K_3 = [1 - 4.38 (\frac{b}{a})^{0.033} (\frac{\rho_1}{\rho_2})^{0.62} (\frac{\Delta Y}{Y_2})]^{1/4}$ $K_4 = 0.0584 (\frac{a}{b}) (\frac{K_1}{K_2})^{0.5} (\frac{\rho_1}{\rho_2})^{1.6} (\frac{\Delta Y}{Y_2})^{1.4}$
Polley and Calus (25)	Brass	Benzene Toluene n-Heptane	1, 3	
Kawasaki et al. (17)	Copper	Benzene Toluene Trichloro-ethylene		$N_u = 0.0295 (Ga Ku Pr)^{1/4} (Re)^{1/2}$
Salov and Danilov (26)		Benzene Toluene Trichlorethylene Heptane Turpentine Gasoline		
Yusufova and Neikdukht (30)		Kerosene		$h \propto (\frac{Q}{A})^{1.26}$

Investigator	Test Surface	Organic Component	Condensation Pattern	Correlation Proposed
Yusufova and Neikdukht (30)	Steel Brass Aluminum	Gasoline		$h \propto \left(\frac{Q}{A}\right)^{1.1}$ $\frac{h}{k} \left(\frac{K}{c_p g}\right)^{1/3} = 0.06 \left(\frac{D}{L}\right)^{0.27} \left(\frac{Q \cdot L}{A \cdot \lambda \cdot g \mu}\right)^{0.36}$
Patterson et al. (23)	Wrought Iron Muntz Metal	Heptane	1	
Hazelton and Baker (15)	Copper	Benzene Toluene Chlorobenzene	1, 3, 5	$h = 79 \left(\frac{a\lambda_1 + b\lambda_2}{aL}\right)^{1/4}$ <p>and</p> $h = 61 \left(\frac{a\lambda_1 + b\lambda_2}{aD}\right)^{1/4}$
Cooper et al. (12)	Copper	Butyl Acetate		
Edwards et al. (13)	Copper	Styrene Butadiene	1	$h = 0.96 \left(\frac{K_1^3 \rho_1^2 g}{\mu_1}\right) \left(\frac{4\Gamma}{\mu_1}\right)^{-0.15}$
Tobias and Stoppel (29)	Brass	Benzene Toluene Cyclohexane Carbontetrachloride n-Heptane		$h = \frac{h_m}{1 - \frac{1}{545} \left[\left(\frac{\Delta\gamma^3 \Delta\rho}{\mu_a^4 g}\right) \left(\frac{M_a b K_b}{M_b a K_a}\right)^{1/2} \right]^{0.21}}$

Investigator	Test Surface	Organic Component	Condensation Pattern	Correlation Proposed
Akers and Turner (1)	Brass	Benzene	1	$h \left(\frac{\mu_1^2}{K_{av}^3 \rho_{av}^2} \right)^{1/3} = 1.47 \left(\frac{4\Gamma}{\mu_1} \right)^{-1/3}$
		Heptane Carbontetra- chloride	3	
Bernhardt (6)	Gold	Freon 112 Freon 113 Perchloroethylene p-xylene	1	$h = 0.8 \frac{a\lambda_1 h_1 + b\lambda_2 h_2}{a\lambda_1 + b\lambda_2}$ $h = h_1 v_1 + h_2 v_2$

APPENDIX C

ROTAMETER CALIBRATION

READING	ML/MIN						
0.1	46.933	5.9	307.718	11.9	575.776	17.9	989.262
0.2	89.045	6.0	310.946	12.0	580.891	18.0	1016.152
0.3	126.677	6.1	314.326	12.1	586.024	18.1	1045.645
0.4	160.159	6.2	317.846	12.2	591.173	18.2	1078.031
0.5	189.811	6.3	321.494	12.3	596.334	18.3	1113.484
0.6	215.920	6.4	325.260	12.4	601.502	18.4	1152.285
0.7	238.762	6.5	329.135	12.5	606.674	18.5	1194.676
0.8	258.619	6.6	333.106	12.6	611.843	18.6	1240.930
0.9	275.734	6.7	337.166	12.7	617.005	18.7	1291.285
1.0	290.326	6.8	341.304	12.8	622.156	18.8	1346.184
1.1	302.642	6.9	345.511	12.9	627.289	18.9	1405.875
1.2	312.869	7.0	349.780	13.0	632.399	19.0	1470.680
1.3	321.211	7.1	354.099	13.1	637.480	19.1	1540.949
1.4	327.872	7.2	358.465	13.2	642.527	19.2	1617.215
1.5	333.001	7.3	362.869	13.3	647.534	19.3	1699.648
1.6	336.787	7.4	367.304	13.4	652.496	19.4	1788.828
1.7	339.348	7.5	371.766	13.5	657.408	19.5	1885.168
1.8	340.842	7.6	376.247	13.6	662.263	19.6	1988.949
1.9	341.394	7.7	380.744	13.7	667.058	19.7	2100.840
2.0	341.142	7.8	385.251	13.8	671.789	19.8	2221.309
2.1	340.178	7.9	389.766	13.9	676.451	19.9	2350.766
2.2	338.630	8.0	394.285	14.0	681.042	20.0	2490.113
2.3	336.589	8.1	398.804	14.1	685.559		
2.4	334.141	8.2	403.323	14.2	689.999		
2.5	331.358	8.3	407.838	14.3	694.364		
2.6	328.338	8.4	412.349	14.4	698.653		
2.7	325.130	8.5	416.855	14.5	702.869		
2.8	321.807	8.6	421.354	14.6	707.013		
2.9	318.423	8.7	425.848	14.7	711.091		
3.0	315.029	8.8	430.336	14.8	715.109		
3.1	311.675	8.9	434.820	14.9	719.075		
3.2	308.398	9.0	439.300	15.0	723.000		
3.3	305.229	9.1	443.776	15.1	726.894		
3.4	302.221	9.2	448.251	15.2	730.773		
3.5	299.382	9.3	452.726	15.3	734.656		
3.6	296.742	9.4	457.204	15.4	738.561		
3.7	294.322	9.5	461.687	15.5	742.512		
3.8	292.142	9.6	466.176	15.6	746.535		
3.9	290.215	9.7	470.674	15.7	750.659		
4.0	288.550	9.8	475.183	15.8	754.919		
4.1	287.158	9.9	479.707	15.9	759.352		
4.2	286.047	10.0	484.246	16.0	764.000		
4.3	285.218	10.1	488.804	16.1	768.906		
4.4	284.676	10.2	493.384	16.2	774.125		
4.5	284.417	10.3	497.985	16.3	779.710		
4.6	284.441	10.4	502.612	16.4	785.725		
4.7	284.748	10.5	507.267	16.5	792.235		
4.8	285.330	10.6	511.950	16.6	799.312		
4.9	286.182	10.7	516.664	16.7	807.035		
5.0	287.300	10.8	521.409	16.8	815.494		
5.1	288.672	10.9	526.187	16.9	824.779		
5.2	290.292	11.0	531.000	17.0	834.995		
5.3	292.150	11.1	535.844	17.1	846.244		
5.4	294.237	11.2	540.724	17.2	858.638		
5.5	296.541	11.3	545.638	17.3	872.309		
5.6	299.052	11.4	550.585	17.4	887.387		
5.7	301.759	11.5	555.565	17.5	904.016		
5.8	304.652	11.6	560.575	17.6	922.344		
		11.7	565.615	17.7	942.555		
		11.8	570.682	17.8	964.813		

APPENDIX D

CALCULATIONS FOR STEAM CONDENSATION

A. Sample Calculations of Experimentally Observed Heat Transfer Coefficients.

Sample Run #15

Heat Load Q = Condensate rate x Enthalpy of condensation

$$= \frac{22 \times 0.967}{454} \times 40 \times 970.3$$

$$\frac{\text{ml/min} \times \text{gm/ml}}{\text{gm/lb}} \times \frac{\text{min}}{\text{hr}} \times \frac{\text{Btu}}{\text{lb}}$$

$$= 2852 \frac{\text{Btu}}{\text{hr}}$$

Condensing surface area A = $\pi/4(\text{Diameter})^2$

$$= \pi/4(5/12)^2$$

$$= 0.1364 \text{ ft}^2$$

Film temperature difference $\Delta t_f = t_{\text{vap}} - t_{\text{surface}}$

$$= 209.0 - 174$$

$$= 35^\circ\text{F}$$

Heat transfer coefficient $h = \frac{Q}{A \Delta t_f}$

$$= \frac{2852}{0.1364 \times 35}$$

$$= 597.4 \frac{\text{Btu}}{\text{hr-ft}^2-^\circ\text{F}}$$

B. Sample Calculations of Predictions of Heat Transfer Coefficients Using Nusselt Equation.

Sample Run #15

Vapor temperature = 209°F

Surface temperature = 174°F

∴ Average condensate film temperature = 191°F

All the film properties are evaluated at 191°F.

$$\text{Thermal conductivity } K_{\ell} = 0.3903 \frac{\text{Btu}}{\text{hr-ft}^2-\text{°F}}$$

$$\text{Density } \rho_{\ell} = 0.967 \frac{\text{gm}}{\text{ml}}$$

$$\equiv 60.3 \frac{\text{lb}}{\text{ft}^3}$$

$$\text{Viscosity } \mu_{\ell} = 0.324 \text{ cp}$$

$$\equiv 0.784 \frac{\text{lb}}{\text{hr-ft}}$$

$$\text{Gravitational acceleration } g = 32.2 \times 3600^2 \frac{\text{ft}}{\text{hr}^2}$$

$$\text{Surface loading } \Gamma = \frac{\text{condensate rate}}{\text{wetted perimeter}}$$

$$= \frac{23 \times (60/454) \times 0.967}{4.25/12}$$

$$= \frac{\text{ml/min} \times \left(\frac{\text{min}}{\text{hr}} \frac{\text{gm}}{\text{lb}} \right) \times \text{gm/ml}}{\text{in} / \frac{\text{in}}{\text{ft}}}$$

$$= 8.3 \frac{\text{lb}}{\text{hr-ft}}$$

Heat transfer coefficient

$$\begin{aligned} h &= 0.924 \left[\frac{K_{\ell}^3 \rho_{\ell}^2 g}{\mu_{\ell} \Gamma} \right]^{1/3} \\ &= 0.924 \left[\frac{0.3903^3 \times 60.3^2 \times 32.2 \times 3600^2}{0.784 \times 8.3} \right]^{1/3} \\ &= 2219.7 \frac{\text{Btu}}{\text{hr-ft}^2-\text{°F}} \end{aligned}$$

APPENDIX E

CALCULATIONS FOR TOLUENE-WATER CONDENSATION

A. Sample calculation of experimentally observed coefficients

Sample run # 46

All liquid properties are evaluated at a mean film temperature of 172°F.

Property	Water	Toluene
Thermal Conductivity K $\frac{\text{Btu}}{\text{hr-ft-}^\circ\text{F}}$	0.3845	0.084
Density ρ $\frac{\text{lb}}{\text{ft}^3}$	60.73	52.65
Enthalpy of Condensation λ $\frac{\text{Btu}}{\text{lb}}$	988	160
Viscosity μ $\frac{\text{lb}}{\text{hr-ft}}$	0.896	0.823

Condensation heat duty for water

$$\begin{aligned}
 Q_w &= \text{condensation rate} \times \lambda \\
 &= \frac{5 \times 0.974}{454} \times 60 \times 988 \\
 &\quad \frac{\text{ml/min} \times \text{gm/ml}}{\text{gm/lb}} \times \frac{\text{min}}{\text{hr}} \times \frac{\text{Btu}}{\text{lb}} \\
 &= 635.9 \text{ Btu/hr}
 \end{aligned}$$

Condensation heat duty for toluene

$$\begin{aligned}
 Q_{\text{tol}} &= \text{condensation rate} \times \lambda \\
 &= \frac{30 \times 0.844}{454} \times 60 \times 160 \\
 &\quad \frac{\text{ml/min} \times \text{gm/ml}}{\text{gm/lb}} \times \frac{\text{min}}{\text{hr}} \times \frac{\text{Btu}}{\text{lb}} \\
 &= 535.4 \text{ Btu/hr}
 \end{aligned}$$

Total heat load

$$\begin{aligned}
 Q_t &= \frac{Q_w + Q_{\text{tol}}}{\text{condensation area}} \\
 &= \frac{635.9 + 535.4}{0.1364} \\
 &= 8587.2
 \end{aligned}$$

Calculation of surface temperature for the middle thermocouple pair

$$T_{\text{front}} = 169.8$$

$$T_{\text{back}} = 167.0$$

$$\begin{aligned}
 T_{\text{surface}} &= T_{\text{front}} + \frac{30}{95} (T_{\text{front}} - T_{\text{back}}) \\
 &= 169.8 + \frac{30}{95} (169.8 - 166.9) \\
 &= 170.7
 \end{aligned}$$

Film temperature $t_f = T_{\text{vap}} - T_{\text{surface}}$

$$= 185.0 - 170.7$$

$$= 14.3 \text{ } ^\circ\text{F}$$

Heat transfer coefficient

$$h = \frac{Q_t}{t_f}$$

$$= \frac{8587.2}{14.3}$$

$$= 600.5 \frac{\text{Btu}}{\text{hr-ft}^2\text{-}^\circ\text{F}}$$

- B. Sample calculations for prediction of heat transfer coefficient using Bernhardt's equation (2.14)

h_w = heat transfer coefficient for water phase

$$= 0.943 \left[\frac{K_\ell^3 \rho_\ell^2 g \lambda}{\mu_\ell D \Delta t_f} \right]^{0.25}$$

$$= 0.943 \left[\frac{(0.3845)^3 (60.73)^2 32.2 (3600)^2}{0.896 (4.25/12) 14.3} \right]^{0.25}$$

$$= 1969.5 \frac{\text{Btu}}{\text{hr-ft}^2\text{-}^\circ\text{F}}$$

h_t = heat transfer coefficient for toluene

$$= 0.943 \left[\frac{K_\ell^3 \rho_\ell^2 g \lambda}{\mu_\ell D \Delta t_f} \right]^{0.25}$$

$$= 0.943 \left[\frac{(0.084)^3 (52.65)^2 32.2 (3600)^2 \times 160}{0.823 (4.25/12) 14.3} \right]^{0.25}$$

$$= 380 \frac{\text{Btu}}{\text{hr-ft}^2\text{-}^\circ\text{F}}$$

$$\begin{aligned}\therefore h_{\text{mean}} &= h_w \times \text{volume fraction of water in condensate} + \\ &\quad h_{\text{tol}} \times \text{volume fraction of toluene in condensate} \\ &= \frac{1969.5 \times 5 + 380 \times 30}{35} \\ &= 607.1 \text{ Btu/hr-ft}^2\text{-}^\circ\text{F}\end{aligned}$$

TABLE III
DATA ON TOLUENE-WATER RUNS

Run #	Condensate rate ml/min		Top		Temperatures °F Middle		Bottom		Vapor
	Water	Toluene	Front	Back	Front	Back	Front	Back	
24	8.00	36.00	143.8	123.1	144.2	144.9	143.8	142.3	183.5
25	5.33	27.33	134.0	118.4	136.5	134.0	134.2	135.6	172.7
26	6.00	30.67	154.5	143.0	154.8	155.7	153.9	155.7	179.4
27	10.50	63.00	154.6	142.1	157.3	155.5	155.0	154.1	186.0
28	4.33	27.00	165.8	158.3	169.4	166.9	167.3	166.7	182.0
29	5.00	37.00	161.1	150.3	164.2	162.1	162.2	161.1	182.1
30	2.33	11.67	113.2	115.1	118.7	131.4	122.8	144.4	166.0
31	4.00	28.00	132.8	115.1	137.0	131.4	136.1	144.4	173.9
32	4.67	23.33	169.7	163.7	171.8	170.3	168.9	169.4	182.3
33	4.00	17.75	168.4	159.1	171.8	168.2	169.8	168.4	181.8
34	7.50	38.25	130.9	119.6	131.9	132.5	130.6	146.1	166.8
35	8.50	35.50	157.9	144.1	161.6	158.5	159.9	157.6	178.2
36	9.00	41.00	159.1	145.4	163.9	161.7	162.2	160.7	184.5
37	5.50	29.50	169.3	162.3	171.2	169.7	169.3	168.9	184.5
38	10.80	52.80	155.1	138.2	157.1	155.6	155.1	154.0	182.9
39	8.00	36.00	154.2	146.8	157.4	155.1	156.3	155.9	179.9
40	6.00	26.00	157.2	148.3	158.9	158.0	157.0	156.7	180.4
41	7.00	29.00	129.4	120.9	130.9	132.7	127.7	133.8	174.6
42	6.50	25.00	156.2	146.9	161.5	157.9	159.8	154.7	183.4
43	7.00	33.00	162.6	153.5	167.5	163.8	163.2	162.8	182.3
44	5.50	27.50	168.7	160.0	171.5	168.4	169.5	168.2	184.9
45	5.20	28.80	169.2	160.9	171.8	169.4	170.3	168.5	185.5
46	5.00	30.00	168.3	159.2	169.8	166.9	168.6	165.9	185.0
47	5.00	29.00	165.0	157.9	167.3	165.5	164.6	164.9	182.9
48	5.00	28.00	164.5	155.8	166.2	162.5	161.7	161.3	179.8
49	5.00	28.00	162.7	155.0	165.1	162.0	159.6	161.4	179.2

VITA

Anil Vasant Gokhale

Candidate for the Degree of

Master of Science

Thesis: CONDENSATION OF MIXTURES GIVING TWO IMMISCIBLE LIQUID
PHASES

Major Field: Chemical Engineering

Bibliographical:

Personal Data: Born in Bombay, India, March 19, 1958, the son
of Mr. and Mrs. V. S. Gokhale.

Education: Graduated from King George English School, Bombay,
India, in May 1974; received Bachelor of Chemical Engineer-
ing degree from University of Bombay in July 1980; completed
requirements for Master of Science degree at Oklahoma State
University in December, 1982.

Professional Experience: Trainee Engineer, Hindustan Petroleum
Corporation, May 1979 to July 1979; graduate teaching and
research assistant, Oklahoma State University, School of
Chemical Engineering, August 1980 to May 1982.